

Radiolarians in Paleoceanography

Selected papers from InterRad XI, Wellington, New Zealand, March 2006

Edited by David Lazarus and Chris Hollis

The Micropaleontology Project, Inc.
New York, 2008

Preface

The six articles in this special issue of *Micropaleontology* were selected from papers presented at the 11th international meeting of radiolarian researchers (InterRad XI), which was held in Wellington, New Zealand, 19-24 March, 2006. Despite being held in a location far from the Northern Hemisphere centers of radiolarian research the conference attracted 120 participants from 19 countries, including 35 participants from Japan. Perhaps the key attractions of this first Southern Hemisphere radiolarian conference, were the well-attended field trips that combined spectacular radiolarian-rich rock successions with pristine natural scenery. The conference was hosted by InterRad, the International Association of Radiolarian Paleontologists, IGCP Project 467, the Subcommittee on Triassic Stratigraphy and GNS Science.

The articles in this special issue illustrate how our understanding of modern radiolarian ecology continues to improve, and demonstrates the application of ecological knowledge to important questions in paleoceanography at various time scales. Six articles in a companion special issue of *Stratigraphy* demonstrate the diverse applications for radiolarian micropaleontology in correlation and geologic dating. The next international radiolarian conference, InterRad XII, will be held in Nanjing, China, in September 2009.

David Lazarus
Museum für Naturkunde
Humboldt Universität zu Berlin, Germany

Chris Hollis
GNS Science New Zealand

Late Quaternary radiolarian assemblages as indicators of paleoceanographic changes north of the subtropical front, offshore eastern New Zealand, southwest Pacific

Vanessa Lüer^{1,2}, Christopher J. Hollis² and Helmut Willems¹

¹University of Bremen, Faculty of Geosciences, PO Box 330 440, 28334 Bremen, Germany

²GNS Science, PO Box 30 368, Lower Hutt, New Zealand

email: vlueer@uni-bremen.de

ABSTRACT: Abundant and diverse polycystine radiolarian faunas from ODP Leg 181, Site 1123 (0-1.2 Ma at ~21 kyr resolution) and Site 1124 (0-0.6 Ma, ~5 kyr resolution, with a disconformity between 0.42-0.22 Ma) have been used to infer Pleistocene-Holocene paleoceanographic changes north of the Subtropical Front (STF), offshore eastern New Zealand, southwest Pacific. The abundance of warm-water taxa relative to cool-water taxa was used to determine a radiolarian paleo-temperature index, the Subtropical (ST) Index. ST Index variations show strong covariance with benthic foraminifera oxygen isotope records from Site 1123 and exhibit similar patterns through Glacial-Interglacial (G-I) cycles of marine isotope stages (MIS)15-1. At Site 1123, warm-water taxa peak in abundance during Interglacials (reaching ~8% of the total fauna). Within Glacials cool-water taxa increase to ~15% (MIS2) of the fauna. Changes in radiolarian assemblages at Site 1124 indicate similar but much better resolved trends through MIS15-12 and 7-1. Pronounced increases in warm-water taxa occur at the onset of Interglacials (reaching ~15% of the fauna), whereas the abundance of cool-water taxa increases in Glacials peaking in MIS2 (~17% of the fauna). Overall warmer conditions at Site 1124 during the last 600 kyrs indicate sustained influence of the subtropical, warm East Cape Current (ECC). During Interglacials radiolarian assemblages suggest an increase in marine productivity at both sites which might be due to predominance of micronutrient-rich Subtropical Water. At Site 1123, an increased abundance of deep-dwelling taxa in MIS 13 and 9 suggests enhanced vertical mixing. During Glacials, reduced vigour of ECC flow combined with northward expansion of cool, micronutrient-poor Subantarctic Water occurs. Only at Site 1123 there is evidence of a longitudinal shift of the STF, reaching as far north as 41°S.

INTRODUCTION

Polycystine Radiolaria are a diverse group of marine microzooplankton, bearing fossilizable skeletons of opaline silica. This fossil group has been used extensively for Quaternary paleoceanographic studies in the Pacific (e.g. Molina-Cruz 1977; Moore 1978; Pisias and Mix 1997; Welling and Pisias 1998), Atlantic (e.g. Morley 1979; Abelmann and Gowing 1997; Dolven et al. 2002), Indian (e.g. Dow 1978; Johnson and Nigrini 1980, 1982) and Southern oceans (e.g. Cortese and Abelmann 2002). Radiolarian depth zonations and the relative abundance of depth restricted taxa can be used for paleoceanographic reconstructions and detection of the influence of certain water masses within a study area (e.g. Casey 1971; McMillen and Casey 1978; Kling and Boltovskoy 1995; Abelmann and Gowing 1997) and to investigate paleoceanographic events (Welling et al. 1996; Wang and Abelmann 2002; Yamashita et al. 2002)

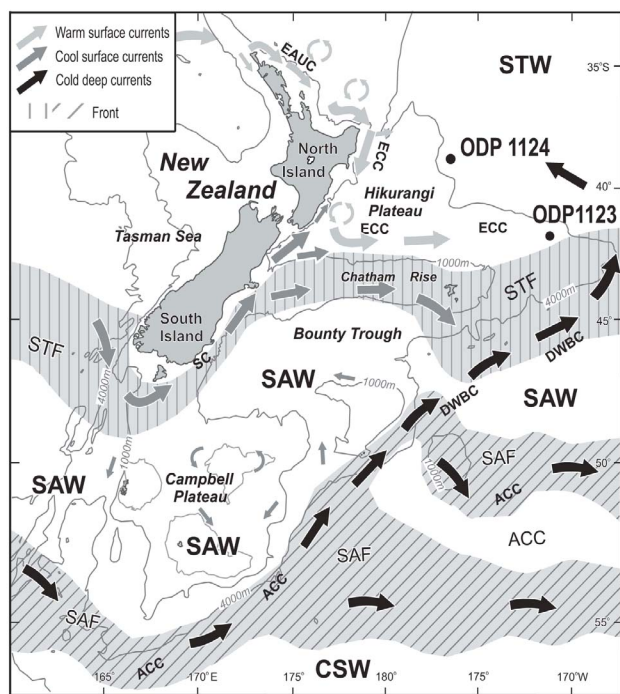
In contrast, there have been very few studies of Quaternary radiolarians (Hays 1965; Petrushevskaya 1967, 1975; Caulet 1986, see also Nelson et al. 1993; Carter et al. 1999b) and their application to paleoceanographic changes in the southern Pacific Ocean (Moore et al. 1978; Hollis et al. 2002; 2006). Our study of radiolarians from sediment cores from north of the STF (ODP Leg 181, Sites 1123, 1124), offshore eastern New Zealand, is the first detailed investigation of Late Quaternary assemblage variation in the region.

The two study locations, Sites 1123 and 1124, lie within a temperate climatic regime east of New Zealand and north of the Subtropical Front (STF). Our quantitative analysis of radiolarian assemblages aims to determine changes in the expression of the STF and associated currents during late Quaternary Glacial-Interglacial (G-I) climate cycles.

OCEANOGRAPHIC SETTING

The Subtropical Front (STF) is a prominent feature of the ocean regime offshore eastern New Zealand (text-fig. 1). It extends to a depth of ~350m (Heath 1976) and appears to have been locked to the Chatham Rise at ~45°S throughout the late Quaternary, including the Last Glacial Maximum (Heath 1985; Nelson et al. 1993; Chiswell 2002; Sikes et al. 2002). In the upper water-mass, however, the front is highly variable in strength. Satellite thermal imaging shows that meanders and eddies form at many different scales (Chiswell 1994). The STF is characterized by a 4-5° C drop in surface temperature and a ~1‰ drop in salinity over 200km (Chiswell 2001; Sikes et al. 2002). It separates high-salinity (~35.7‰), macronutrient-poor (nitrate, dissolved reactive phosphorus, silica), micronutrient-rich (iron and other trace metals), warm (>15°C summer) Subtropical Water (STW) from southern Subantarctic Water (SAW), which has lower salinity (~34.5‰), is macronutrient-rich, micronutrient-poor and cool (<15°C summer; Heath 1985; Nelson et al. 2000; Chiswell 2001, 2002). The high amount of micronutrients in STW triggers high primary production, especially in summer (Boyd et al. 2004). High nitrate, low chlorophyll (HNLC) SAW has low primary production with little seasonal variation (Boyd et al. 2004). The southern boundary of SAW is defined by the Subantarctic Front (SAF), which follows the submarine escarpment of Campbell Plateau (text-fig. 1). The SAF defines the northern extent of the Southern Ocean and Antarctic Circumpolar Current (ACC) and is associated with another drop in temperature of ~2°C and annual mean surface-water temperature of <10° C to the South. It restricts macronutrient-rich Circumpolar Subantarctic Water (CSW) to latitudes >55°S (Carter et al. 1999b).

The shallow subtropical East Cape Current (<350m; ECC) is a continuation of the East Australian Current (EAUC) that flows



TEXT-FIGURE 1
Location of ODP Sites 1123 and 1124 (black dots) and distribution of major water masses, currents and fronts offshore eastern New Zealand. CSW, Circum-Antarctic Surface Water; SAW, Subantarctic Surface Water; STW, Subtropical Surface Water; EAUC, East Australian Current; ECC, East Cape Current; SC, Southland Current; ACC, Antarctic Circumpolar Current; DWBC, Deep Western Boundary Current; STF, Subtropical Front; SAF, Subantarctic Front (modified from Carter 2001).

southward along North Island's east coast as a series of eddies before turning east at 2°S to follow the northern flank of Chatham Rise (Nelson et al. 2000; text-fig. 1). South of the STF, the cool shallow Southland Current (SC) flow travels around the bottom of South Island before turning northward (text-fig. 1). It is associated with the narrow Southland Front (SF), the landward expression of the STF that separates relatively warm, salty STW on the continental shelf from cool, relatively fresh SAW offshore (Sutton 2003). On its way north the SC mixes with offshore SAW on Campbell Plateau comprising ~90% SAW and ~10% STW before most of its flow is deflected to the east, south of Chatham Rise, while filaments of the SC pass through Mernoo Gap to combine with the ECC (Sutton 2003; text-fig. 1).

The remaining major current in this region is the Deep Western Boundary Current (DWBC), which separates from the Antarctic Circumpolar Current (ACC) at the SAF and flows northward, along the New Zealand continental margin (text-fig. 1). The DWBC has an upper boundary of 2000m (Carter et al. 1999a, b) and is a major component in the global ocean thermohaline circulation system, supplying 40% of the cold, saline Antarctic bottom water to the major ocean basins through the Pacific Ocean (Warren 1981). It is believed to have had a significant influence on the Earth's heat budget since its inception ~33 Ma (Clarke et al. 2001). The DWBC contains a mixture of Antarctic Bottom Water (AABW) and North Atlantic Deep Water (NADW; Carter et al. 1999b; Hall et al. 2001). These waters are entrained and mixed by the west wind-driven ACC to form Circumpolar Deep Water (CDW; Carter et al. 1999b).

The two study sites lie within STW north of the STF and have the potential to record variations in the influence of the ECC and STF in shallow waters and of the DWBC at depth.

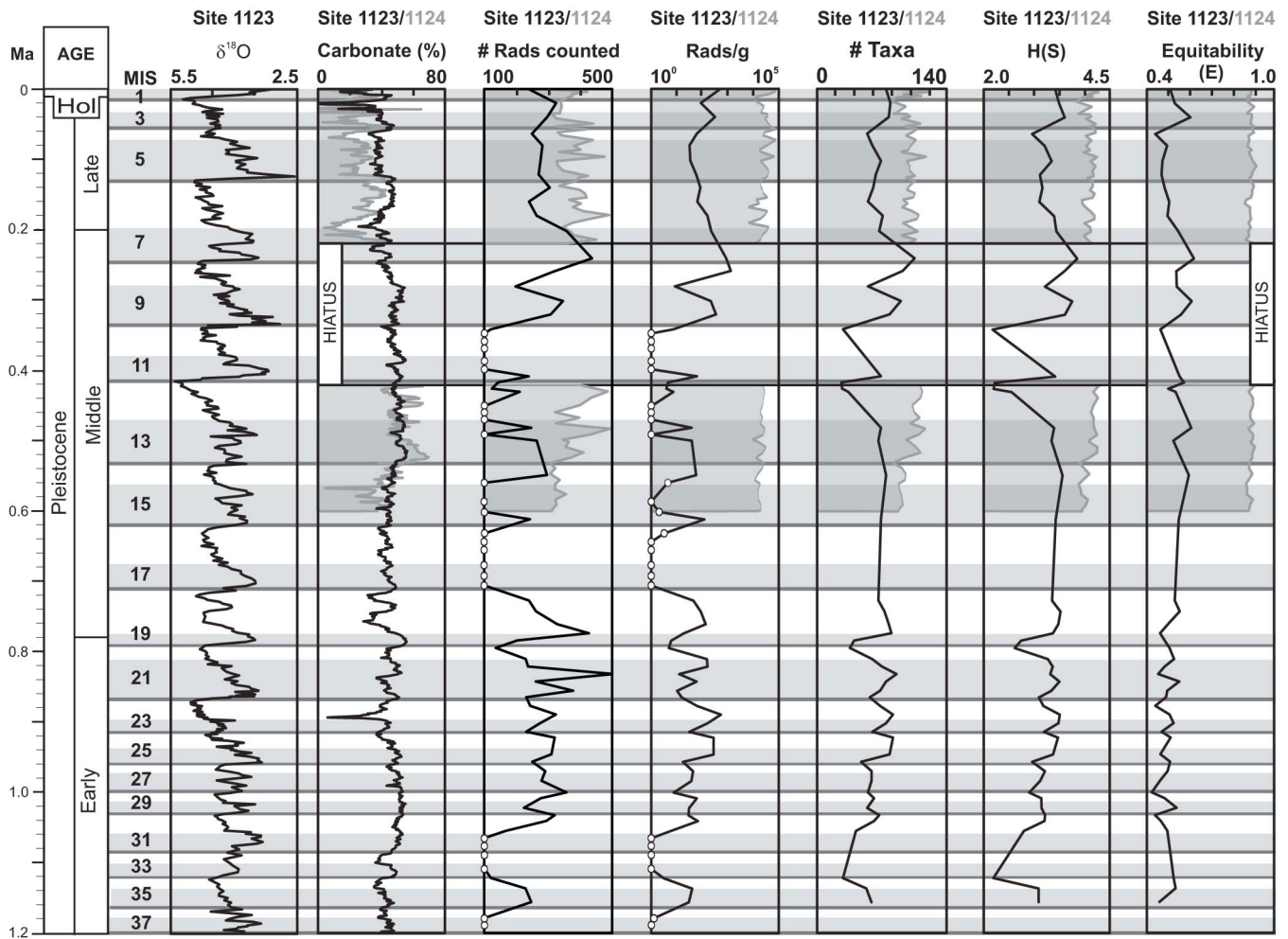
MATERIAL AND METHODS

Sediment samples and chronological framework

Sites 1123 (41°47'S; 71°30'W, 3290m water depth; text-fig. 1) and 1124 (39°30'S; 176°32'W, 3960m water depth) were APC/XCB cored during ODP Leg 181 (Carter et al. 1999b). Sediments of both cores consist of clayey nannofossil ooze, nannofossil ooze, nannofossil silty clay and intercalated tephra layers. Magnetic susceptibility and color reflectance records were used to identify overlapping intervals in Site 1123 Holes B and C, and Site 1124 Holes A-D in order to establish a continuous sedimentary record. Depths are based on these spliced records and are recorded as meters composite depth (mcd). Both sites have near complete Neogene records. In this study we provide an overview for the last 1.2 Myrs based on Site 1123 (based on Lüer 2003) and then compare records for the last 600 kyrs for both sites. 10 cc samples were taken every ~0.6 mcd (Site 1123) and ~0.36 mcd (Site 1124) to provide a temporal resolution of ~21 kyrs (Site 1123) and ~5 kyrs (Site 1124), respectively, during the last 600 kyrs. Unfortunately, Site 1124 has a hiatus at 0.42-0.22 Ma (Carter et al. 1999b; Hall et al. 2002; Aita and Suzuki 2003; Fenner and DiStefano 2004). For Site 1123 an orbitally tuned timescale was developed from benthic foraminiferal oxygen isotope records (Hall et al. 2001). The age model for Site 1124 is based on graphical correlation of color reflectance data with the record from Site 1123 (Hall et al. 2002). Two Late Quaternary radiolarian bioevents recorded in this study, the last occurrences of *Stylatractus universus* at 0.42 Ma and *Eucyrtidium calvertense* at 0.48 Ma, are in good agreement with previous studies (Hays and Shackleton 1976; Morley and Shackleton 1978; Lazarus 1992; Shackleton et al. 1995; Sanfilippo and Nigrini 1998; Aita and Suzuki 2003).

Sample processing

Because processing techniques were developed and refined in the course of this project, there are specific differences in the processing methodologies used for the two sites, especially in relation to the drying of sediments and residues, use of mesh size and the technique of strewn slide production. For Site 1123, we prepared strewn slides from a >63 µm fraction of oven-dried residue (see Appendix 3 for details). This method allowed comparison with the shipboard samples, which were prepared by this method (Carter et al. 1999b). However, because most paleoceanographic studies of Quaternary radiolarians are based on smaller size fractions (e.g. Wang and Abelmann 1997; Yamashita et al. 2002), the >45 µm fraction was analysed for Site 1124 to allow better comparison with other studies. In addition, samples were freeze-dried (Abelmann 1988) to reduce breakage of delicate radiolarian tests (Itaki and Hasegawa 2000) and a wet settling technique was adopted to ensure random distribution of radiolarian tests on the slides (Moore 1973; Abelmann 1988; Abelmann et al. 1999). A newly developed mounting technique was used to avoid the formation of air bubbles, especially within radiolarian tests. See Appendix 3 for details of processing methods. It is recognized that these differences in processing present problems in comparing assemblage data between the two sites. Diversity is expected to be greater at Site 1124, simply because of gentler drying methods and use of a smaller sieve size. A smaller sieve



TEXT-FIGURE 2

General features of radiolarian assemblages from ODP Site 1123 (0-1.2 Ma, black line) and Site 1124 (0-0.6 Ma, shaded grey) with benthic foraminiferal $\delta^{18}\text{O}$ record for Site 1123 and colour reflectance for Sites 1123 and 1124 for reference (from Hall et al. 2001, 2002): number of radiolarians counted in each sample (# Rads counted); radiolarians per gram of sediment (Rads/g), taxic richness (# Taxa), diversity (H(S)) and Equitability (E). Sparse samples (<100 specimens/sample) are shown as unfilled circles. Marine Isotope Stages (MIS) are calibrated according to the $\delta^{18}\text{O}$ and reflectance records at Site 1123. Glacial terminations are shown as dark grey horizontal lines and Interglacial Stages are shaded light grey. A hiatus at Site 1124 extends from uppermost MIS12 to mid-MIS7.

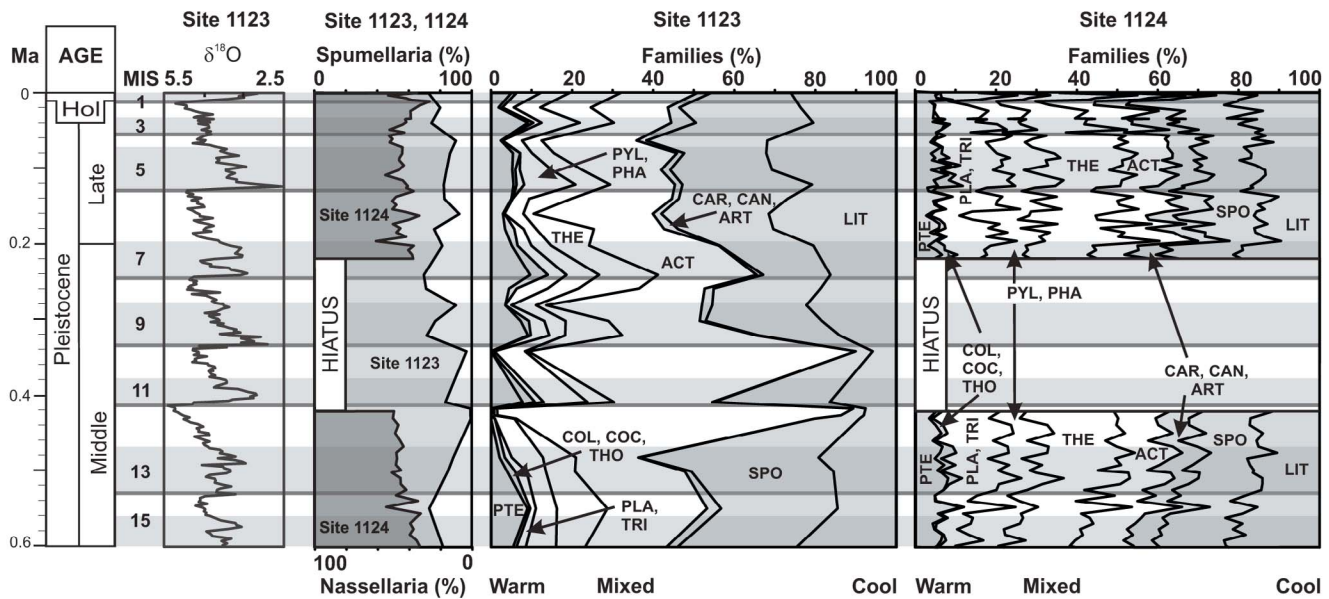
size is also expected to increase the diversity and abundance of nassellarians, which tend to be smaller than spumellarians

This study is based on the analysis of 151 samples, 79 from Site 1123 and 72 from Site 1124. The taxonomic level of counting groups ranges from subspecies to undifferentiated family and suborder categories. Generally, in case of incomplete or broken tests only radiolarians with >50% of the test preserved were counted. For nassellarians, only specimens with a cephalis present were counted. The ratio of radiolarian fragments over the total of counted specimens was used as a guide to radiolarian preservation within individual assemblages.

Bulk samples, radiolarian residues and strewn slides are stored and catalogued at GNS Science, Lower Hutt, New Zealand, (Site 1123) and at the University of Bremen, Germany (Site 1124). Raw data files are available at www.pangaea.de, an online archive for marine environmental scientific data.

Statistical analysis

For both sites we aimed for a minimum count of 300 specimens per sample in order to provide statistically significant abundance estimates (Cortese 2004). For Site 1123 we were not able to reach this number owing to the scarcity of radiolarians in some intervals. For our statistical analysis we included all samples with >100 specimens because, although errors are relatively large in counts of <300 specimens, general features of the assemblages are still meaningful (e.g. diversity, abundance of common species). Hayward et al. (1999) have established that counts of 100 specimens provide an adequate guide to general faunal character because the main statistical methods are primarily influenced by the abundance variations within the most common taxa. Diversity indices were calculated using a public domain data analysis software package, PAST (Paleontological Statistics; Hammer et al. 2001), including taxic richness (S = number of taxa in individual samples), Fisher α Index (α), Shannon-Wiener Information Function (H(S)) and Equitability (E). The linear coefficient



TEXT-FIGURE 3

Abundance of radiolarian orders (spumellarians, nassellarians) and families during the last 600 kyrs at ODP Sites 1123 and 1124 with benthic foraminiferal $\delta^{18}\text{O}$ record for reference (Hall et al. 2001). Warm-water affinities (shaded to left): Collosphaeridae (COL), Coccodiscidae (COC), Tholoniidae (THO), Pterocoryidae (PTE). Cool-water affinities (shaded to right): Spongodiscidae (SPO), Litheliidae (LIT), Carpaniidae (CAR), Can-nobotryidae (CAN), Artostrobiidae (ART). Mixed affinities: Actinommididae (ACT), Pyloniidae (PYL), Phacodiscidae (PHA), Theoperidae (THE), Plagoniidae (PLA), Trissocyclidae (TRI). Other shading and symbols as for text-figure 2.

of correlation (r ; Godfrey et al. 1988; Bevington and Robinson 1991) was used to examine patterns of covariance within radiolarian assemblage data and between radiolarian associations and paleoclimate proxies, such as oxygen isotopes (Hall et al. 2001, 2002).

Radiolarian paleotemperature and paleodepth indicators

Radiolarian assemblages at the two sites consist of a mixture of mainly transitional, subtropical and subantarctic species typical of temperate waters (Boltovskoy 1987) and transitional subzones TR1-3 of Hollis and Neil (2005). Based on local biogeographic data (Moore 1978; Boltovskoy 1987; Hollis and Neil 2005) 93 paleotemperature indicator species were identified (Appendix 1). These include 54 warm-water (tropical-subtropical) species and 33 cool-water (antarctic-subantarctic) species. Six taxa are considered to typify the transitional zone. The abundance of warm-water species relative to cool-water species was used to define the Subtropical Index (ST Index):

Subtropical (ST) Index: warm-water taxa [%]/cool-water taxa [%]

To examine water column structure radiolarians were also classified by depth zones utilising established depth zonations (Renz 1976; McMillen and Casey 1978; Kling 1979; Boltovskoy and Jankilevich 1985; Kling and Boltovskoy 1995; Abelmann and Gowing 1997). In this study radiolarian species that are restricted to the upper 100m of the water column or that have peak abundance at 100m are characteristic surface and subsurface dwellers and are classified as shallow dwellers. Deep-dwelling radiolarians are those that have their greatest abundance at >100m water depth and include species that are most abundant in intermediate watermasses (c. 200m) as well as those most abundant in deep waters (>300m). Altogether, 75 species were assigned to depth zones and 47 were classified as shallow dwellers whereas 28 were classified as deep-dwelling species (Appendix 1). It is

noted, however, that some radiolarians occur at different water depths in different latitudinal zones. Many radiolarian species that are classified as shallow-dwelling, cool-water species in high latitude surface waters are deep-dwelling species in lower latitudes (Casey 1971). For this reason, in the following section we are careful to rule out changes in water temperature as a cause for faunal changes prior to considering possible changes in water column structure or vertical mixing.

RESULTS

Variations in radiolarian abundance, diversity and preservation

Abundance and diversity are relatively high at Sites 1123 and 1124, which is consistent with the occurrence of rich radiolarian faunas in the transitional southwest Pacific, north of the STF (Hollis and Neil 2005). Overall, abundance is much higher at Site 1124 than at Site 1123, with maxima of ~70,000 and ~1,300 radiolarians per gram sediment (rads/g) and means of ~26,000 and ~100 rads/g, respectively (text fig 2). Diversity is also much higher at Site 1124, with a maximum of 122 vs 101 (Site 1123) taxa and averages of 98 and 53 taxa per sample (Site 1123), respectively. This marked difference is partly an artefact of differences in processing. In particular, the use of a 45 μm sieve, freeze-drying of samples and wet-mounting of residues are all likely to improve the recovery of radiolarians. However, other preservational differences and the very sparse assemblages in some intervals at Site 1123 indicate that these methodological differences serve to accentuate actual differences. Assemblages from Site 1124 are consistently richer, more diverse and better preserved than those from Site 1123. Radiolarians are mostly well- to very well-preserved at Site 1124, whereas preservation is much more variable at Site 1123 and ranges from poor, especially characterized by high fragmentation of radiolarian tests, to moderate and good to very good. Three samples from Site

1123 contain reworked Paleogene radiolarian specimens (1123B-3H-5, 126-128 cm; 1123B-6H-2, 19-23 cm; 1123C-5H-6, 17-21 cm).

Radiolarians from Site 1123 are generally rare to common, with most samples containing >500 radiolarians/g (text-fig. 2). Two intervals of low abundance are noted: near the base of the studied interval (MIS37-31) and in the middle Pleistocene (MIS17-10). Many of the sample residues from these two intervals contain <100 specimens (text-fig. 2) and, for this reason, these samples are not used for quantitative faunal analysis. A total of 163 taxa were recorded in samples from this site and assemblages are moderately diverse (maximum H(S) = 3.9; mean H(S) = 3.2; text-fig. 2). Equitability is also moderate to high (E = 0.4-0.6). Significant correlation between radiolarian abundance, diversity and oxygen isotopes was determined for samples from Site 1123 (Appendix 2). Generally, abundance and diversity tend to be highest at G-I transitions and decrease in Glacials, except in MIS31-30, 19-18 and 9-8, where the pattern is reversed (text-fig. 2).

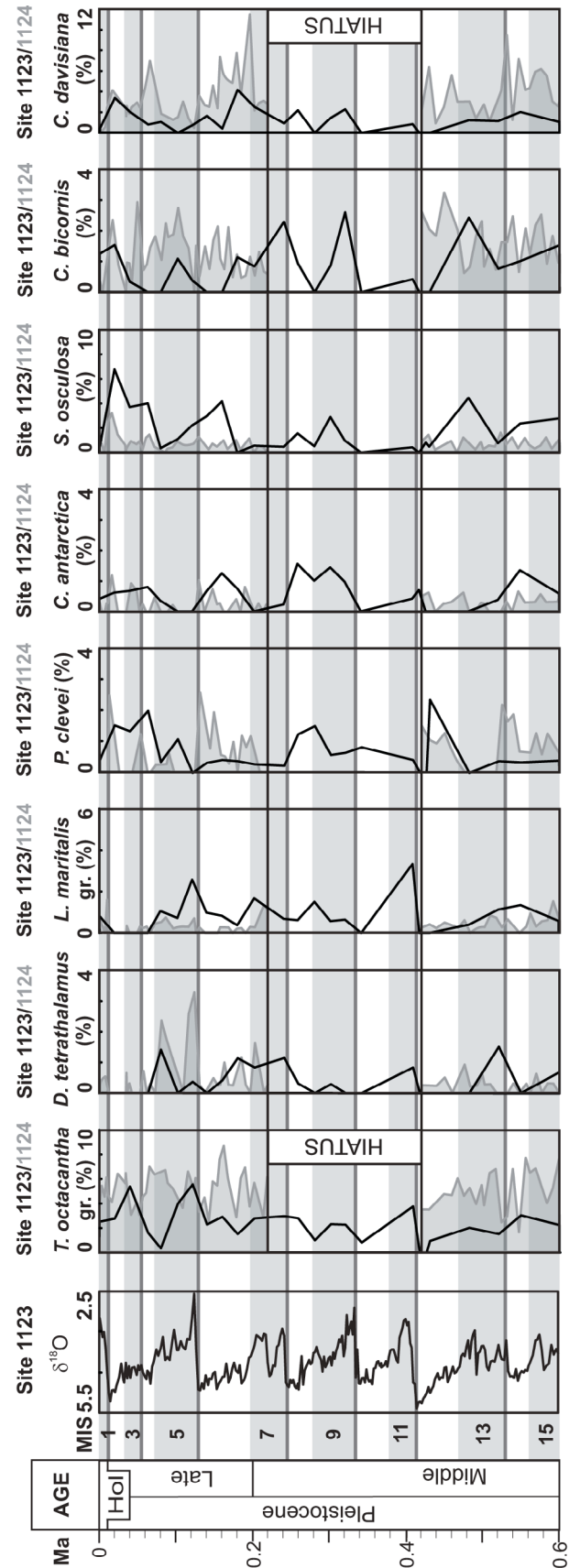
To examine the degree of covariance between radiolarian assemblage characteristics and global climatic changes we determined correlation coefficients for assemblage parameters and oxygen isotope values (Hall et al. 2001; 2002) for the same samples from Site 1123 (Appendix 2a, b). Although, significant positive correlations are evident between diversity parameters and abundance, only diversity exhibits a significant negative correlation with $\delta^{18}O$. From this pattern of covariance we infer that oceanographic changes, e. g. local changes in water temperature (e.g. Pahnke and Sachs 2006; Crundwell et al. in press) at this site during G-I cycles had greatest impact on radiolarian diversity, with a discernable but statistically insignificant effect on abundance. Specifically, radiolarian diversity increases in most Interglacials and is especially pronounced in the later Interglacials (MIS11 to MIS3).

Radiolarians are very abundant and very diverse at Site 1124 (text-fig. 2). A total of 271 taxa were recorded and diversity is significantly higher than at Site 1123 (maximum H(S) = 4.3; mean H(S) = 4.0). Taxa are also much more evenly distributed within assemblages than at Site 1123 (mean E = 0.89). The higher diversity, and possibly the higher Equitability, is probably due in part to processing differences (see above). In comparison with Site 1123, there is much less variation in abundance and diversity at Site 1124. Apart from distinct baseline increases in diversity at the bases of MIS13 and MIS1 (text-fig. 2), there is no obvious relationship between abundance and diversity parameters and G-I cycles.

As for Site 1123, abundance and diversity parameters are positively correlated although a significant correlation is not observed for abundance and Equitability (Appendix 2c). This is because Equitability is higher and less variable at Site 1124, compared to Site 1123. No $\delta^{18}O$ data are available for Site 1124.

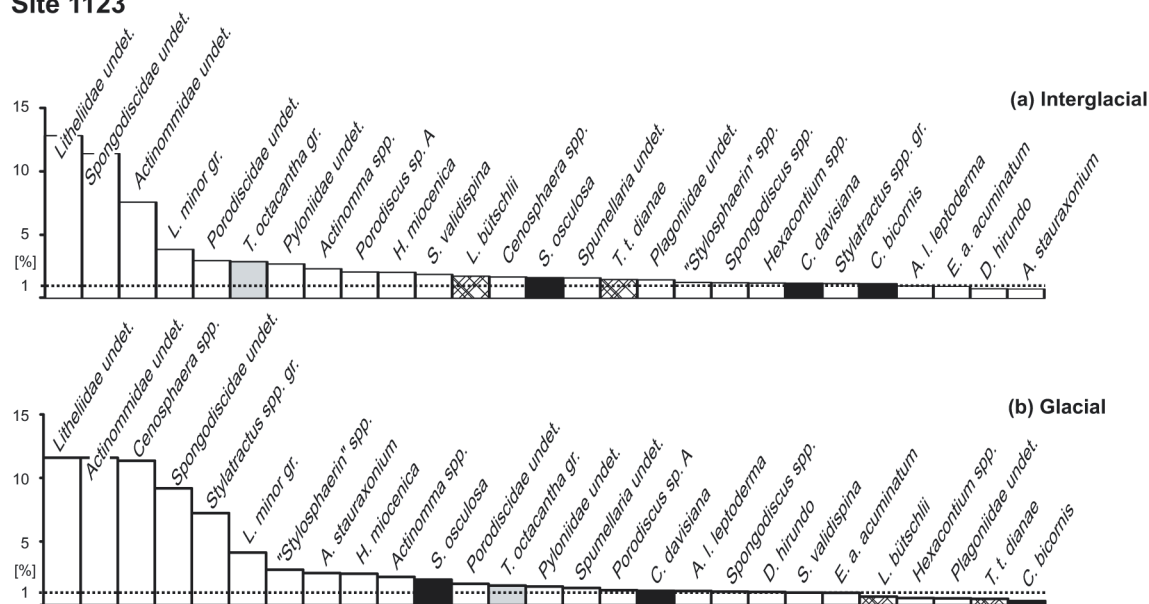
Radiolarian assemblage variation: orders and families

Spumellarians dominate radiolarian assemblages at Site 1123 (70-99.5%) and are slightly more common than nassellarians at Site 1124 (40-74%; text-fig. 3). This is typical of temperate South Pacific faunas (Boltovskoy 1987; Hollis and Neil 2005). The higher abundance of nassellarians at Site 1124 is due mainly to the greater abundance of small nassellarians (45-63 gm) and the better preservation of fragile nassellarian tests due to gentler preparation methods.

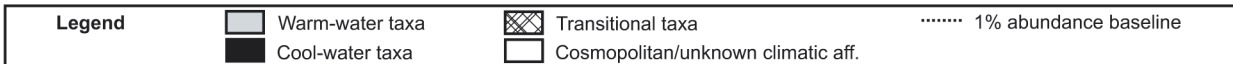
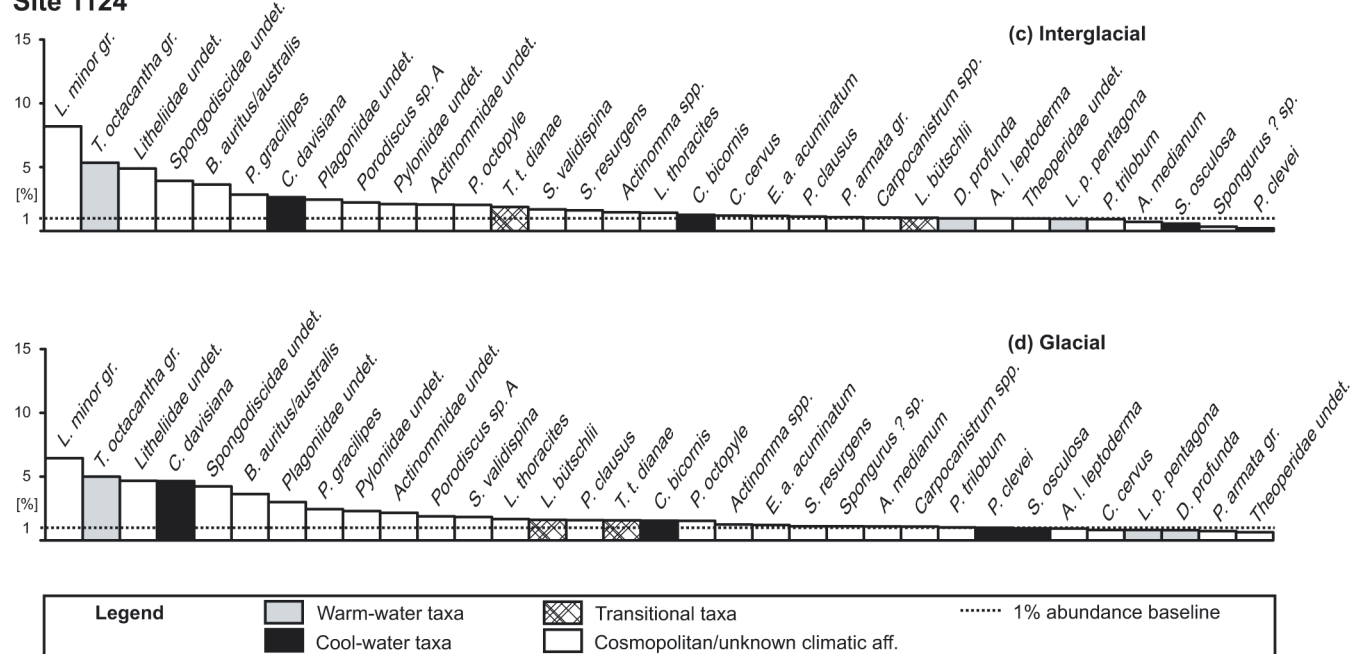


TEXT-FIGURE 4
Abundance of selected radiolarian taxa at ODP Sites 1123 (black line) and 1124 (shaded grey) during the last 600 kys with benthic foraminiferal $\delta^{18}O$ record for reference (Hall et al. 2001). Other shading and symbols as for text-figure 2.

Site 1123



Site 1124



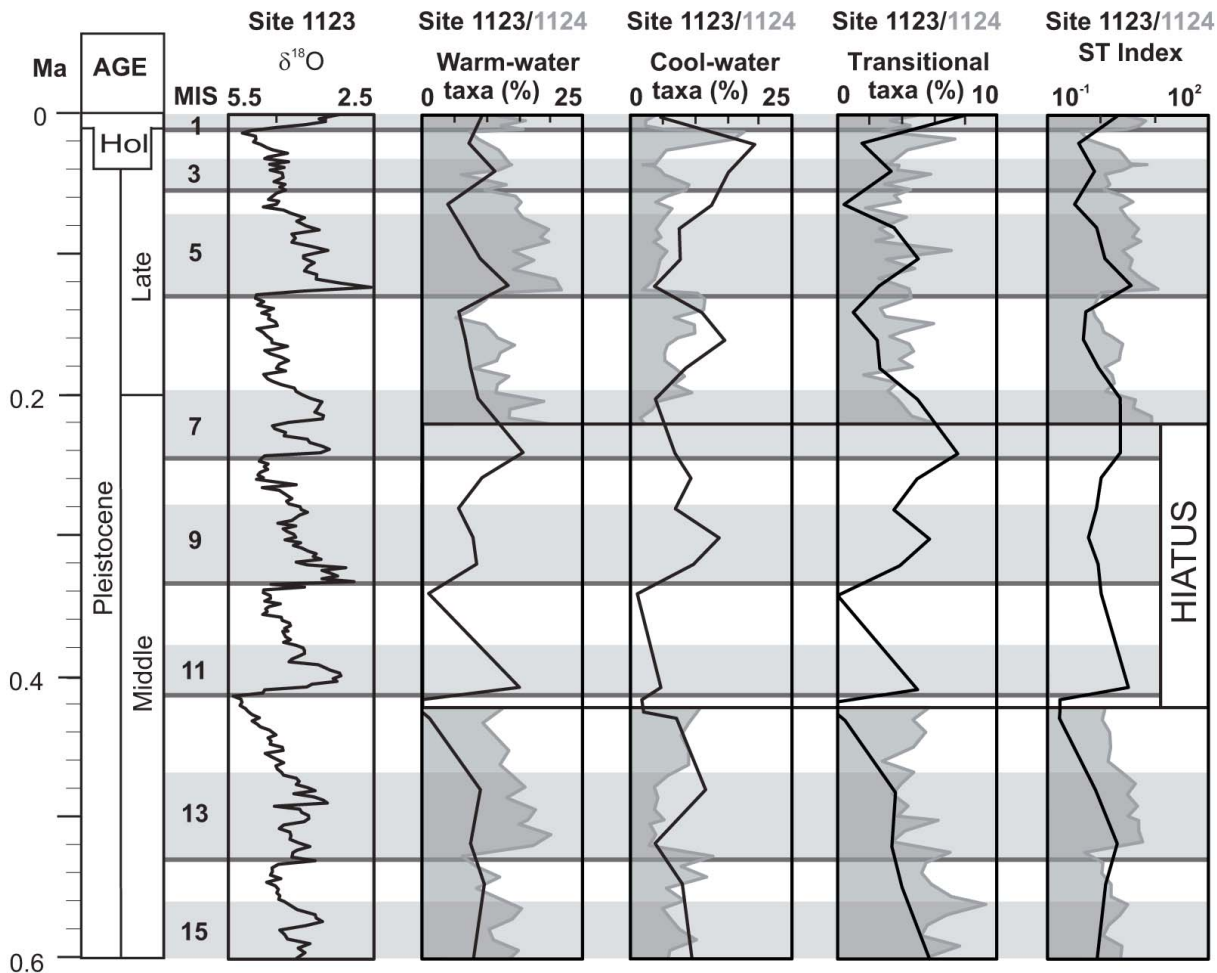
TEXT-FIGURE 5

Average frequency histograms for common taxa (>1%) and significant marker taxa (<1%) within Interglacial (a) and Glacial (b) samples at ODP Site 1123 and within Interglacial (c) and Glacial (d) samples at Site 1124.

Actinommiids, spongodiscids and litheliids are the most abundant spumellarian families at both sites (text-fig. 3). Average values for each family are at least 20% at Site 1123 and 12% at Site 1124, which is consistent with observations on Recent distribution patterns in surface sediments in the southwest Pacific (Boltovskoy 1987; Hollis and Neil 2005). Pyloniids, which are common in Recent radiolarian assemblages north of the STF (Boltovskoy 1987; Hollis and Neil 2005) average to 5% at Site 1123 and 10% at Site 1124. Collosphaeridae, Phacodiscidae, Coccodiscidae and Tholonidae are rare at both sites. Collosphaerids, phacodiscids, coccodiscids and, at Site 1124, tholoniids, are never more

abundant than 2.5% at Site 1123 and 3.5% at Site 1124. Generally, collosphaerids, coccodiscids and phacodiscids are rare in the transitional southwest Pacific (Boltovskoy 1987) and in the eastern New Zealand area (Hollis and Neil 2005).

Pterocoryids and theoperids dominate Recent nassellarian assemblages north of the STF (Boltovskoy 1987; Hollis and Neil 2005). With an average of 8% (Site 1123) and 19% (Site 1124), respectively, theoperids are the most common nassellarians in the study area (text-fig. 3). Pterocoryids, plagoniids, arstostrobids, and at Site 1124, trissocyclids, are also common (>5%). Car-



TEXT-FIGURE 6
Abundance of paleotemperature indicators at ODP Sites 1123 (black line) and 1124 (shaded grey) during the last 600 kyrs with benthic foraminiferal $\delta^{18}\text{O}$ record for reference (Hall et al. 2001). The Subtropical (ST) Index is the ratio of warm- to cool-water taxa. Other shading and symbols as for text-fig. 2.

ponaniids exceed 1% (Site 1123) and 3% (Site 1124) in individual samples. While cannobotryids are >1% in most assemblages at Site 1124, the family is very rare at Site 1123 (text fig. 3). The higher abundance of these small nassellarians at Site 1124 is due to the better preservation and incorporation of smaller radiolarian tests (>45 μm).

Variation within G-I cycles at Sites 1123 and 1124 are very similar. Spumellarian collosphaerids, coccodiscids, tholoniids and nassellarian pterocoryids have increased abundance in Interglacials indicating that these families are dominated by warm-water taxa (text-fig. 3). Radiolarian assemblages within Glacials are dominated by spongodiscids and litheliids and have increased abundance of carpocaniids, cannobotryids and artostrobiids indicating the dominance of cool-water taxa within these families (text-fig. 3). Abundance trends of all other families show mixed affinities, including a mixture of warm- and cool-water species.

Radiolarian assemblage variation: key species and species groups

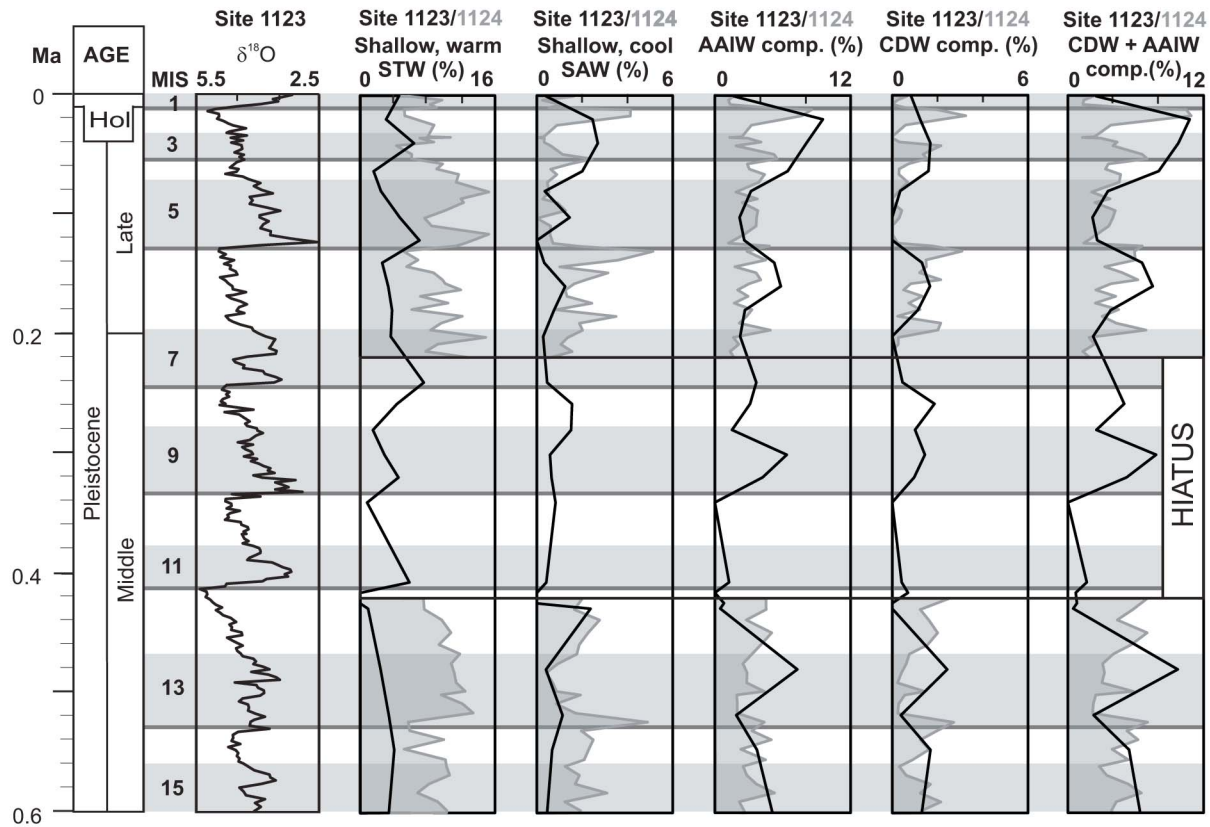
Abundance variations in key paleoenvironmental indicator species are used to further examine the changes in oceanographic conditions through the climate cycles identified at the two sites (text-fig. 4). Comparison of abundance variations between the

two sites also helps to clarify the effects of the different processing methodologies.

***Tetrapyle octacantha* group**

Tetrapyle octacantha gr. includes species of *T. octacantha* and *Octopyle stenozona*. Plankton and surface sediment studies identify peak abundances of *T. octacantha* gr. in the tropical (Renz 1976, Moore 1978; Boltovskoy and Jankilevitch 1985) and subtropical (Molina-Cruz 1977) Pacific. Moore's (1978) tropical factor is clearly dominated by this species group. Boltovskoy (1987) recorded highest abundance of *T. octacantha* gr. in the subtropical and tropical zones. Lombardi and Boden (1985) documented peaks of *T. octacantha* gr. in the tropical Pacific as well as in the vicinity of the Subtropical Front (STF). Hollis and Neil (2005) found higher abundance of *T. octacantha* gr. in Subtropical Water (STW), north of the STF. In the modern ocean *T. octacantha* gr. lives in shallow water masses and is most abundant in the upper 50m of the water column (e.g. Renz 1976; McMillen and Casey 1978; Kling 1979; Kling and Boltovskoy 1995).

At Site 1123, *T. octacantha* gr. abundance tends to increase in Interglacials (text-fig. 4), a feature that is corroborated by a significant negative correlation with the oxygen isotope record (r



TEXT-FIGURE 7

Abundance of radiolarian depth indicators at ODP Sites 1123 (black line) and 1124 (shaded grey) during the last 600 kyr with benthic foraminiferal $\delta^{18}\text{O}$ record for reference (Hall et al. 2001). Depth categories are shallow, warm Subtropical Surface Water (STW); shallow, cool Subantarctic Surface Water (SAW); Circumpolar Deep Water (CDW); Antarctic Intermediate Water (AAIW) components, and combined CDW and AAIW (deep, cool southern-sourced waters).

= -0.444; $r \geq 0.396$ is significant at $P = 0.05$, $N = 25$). A small peak in Glacial stage MIS8 is consistent with other indications, as discussed below, that this single sample has clear warm-water affinities. *T. octacantha* gr. also tends to be most common in Interglacials at Site 1124 although abundance peaks are recorded in Glacial stages MIS6, 4 and 2 (text-fig. 4). The reasons for these peaks are uncertain but they may reflect warming pulses within the Glacials or other oceanographic factors. In general, the abundance variation of *T. octacantha* gr. is in good agreement with the established species' ecology, i.e. a shallow-dwelling species that can be used to detect influences of STW and ECC flows. The higher abundance of *T. octacantha* gr. at Site 1124 reflects the stronger influence of these water masses at this site, particularly in Glacial stages in the late Pleistocene. Test sizes of individual specimens of the *T. octacantha* gr. included in this study are $>63\mu\text{m}$ and differences in the processing methods are expected to be minor.

Didymocyrtis tetrathalamus

D. tetrathalamus is very abundant in surface sediments in tropical to subtropical waters of the Pacific Ocean (Renz 1976; Molina-Cruz 1977; Moore 1978; Boltovskoy and Jankilevich 1985; Lombardi and Boden, 1985; Boltovskoy 1987) and is present north of the STF in the eastern offshore New Zealand area (Hollis and Neil 2005). The species is a shallow-water dweller, mainly living within the upper 50m of the water column (e.g. McMillen and

Casey 1978; Kling 1979; Kling and Boltovskoy 1995).

At Site 1123, *D. tetrathalamus* is common within Interglacials but is not recorded in Glacials, apart from rare occurrences in MIS8 and 6 (text-fig. 4). *D. tetrathalamus* occurs in both Interglacials and Glacials at Site 1124, except it is absent from MIS2. This species is most abundant in Interglacials and peaks in MIS5 (text-fig. 4). Due to its abundance within Interglacials at both sites, *D. tetrathalamus* is considered to be a reliable warm-water indicator, which agrees with the known species ecology. *D. tetrathalamus* has a weak negative correlation with oxygen isotopes at Site 1123 which is probably due the general scarcity ($<2\%$) of this species at this site ($r = -0.331$). *D. tetrathalamus* is used to indicate warm, shallow water masses of STW and ECC, herein. The impact of the different processing methods is believed to be minor because the species is generally larger than $63\mu\text{m}$ and has a relatively robust test.

Lamprocyclus maritilis group

The species included in the *Lamprocyclus maritilis* gr. are *L. maritilis maritilis* and *L. maritilis polypora*. *L. m. maritilis* is a common element of the tropical and subtropical zones whereas *L. m. polypora* is more abundant in the transitional zone of the southwest Pacific area according to Boltovskoy (1987). In the eastern New Zealand region both subspecies are common in surface sediments north of the STF, signaling their warm-wa-

TAXA	Ref 1	Comments	Site	Mor78	Bol87	sp. ID	H&N05 Temp	depth	Ref 2
COOL									
<i>Acanthosphaera pinchuda</i> Boltovskoy & Riedel	Bol 98		1		SA	19	cool		
<i>Acrosphaera arktios</i> (Nigrini)	N&M 79	As <i>Polysolenia</i>	1, 2				SA	cool	
<i>Actinomma antarcticum</i> (Haeckel)	N&M 79		1, 2		AA	20	SA	cool	surface 4,5
<i>Actinomma delicatulum</i> (Dogiel)	N&N 82		1				SA	cool	
<i>Androcyclas gamphonycha</i> (Jørgensen)	N&M 79	Includes <i>Lamprocyrtis</i> <i>? hammai</i> (Campbell & Clark) in N&M 79	1, 2		SA	172	SA	cool	deep 3
<i>Antarctissa cylindrica</i> (Petrushevskaya)	N&N 82		1, 2				SA	cool	
<i>Antarctissa denticulata</i> (Ehrenberg)	N&M 79		1, 2	AA-SA	AA	116	SA	cool	
<i>Antarctissa strelkovi</i> Petrushevskaya	Pet 67		1	AA-SA	AA	116		cool	surface 5
<i>Artostrobos annulatus</i> (Bailey)	Pet 67		1		SA	183		cool	
<i>Botryostrobos aquilonaris</i> (Bailey)	Bol 98		1, 2	SA	SA	184	SA	cool	deep 3
<i>Cenosphaera cristata?</i> Haeckel	N&M 79		1, 2	C-SA	AA	30	SA	cool	
<i>Cromyechinus antarctica</i> (Dreyer)	Bol 98		1, 2		AA	36	SA	cool	deep 5
<i>Cycladophora bicornis</i> (Popofsky)	N&M 79	As <i>Theocalyptra</i>	1, 2		C	165	SA	cool	intermediate 2,3,5
<i>Cycladophora davisiana</i> (Ehrenberg)	Bol 98		1, 2		C	165	SA	cool	intermediate 3,4
<i>Dictyophimus bicornis</i> (Ehrenberg)	Pet 67		1		AA	140		cool	
<i>Lithelius nautiloides</i> Popofsky	Bol 98		1, 2		AA	96	SA	cool	
<i>Peripyramis circumtexta</i> Haeckel	Bol 98		1, 2		SA	159	SA	cool	deep 3
<i>Phormacantha hystrix</i> (Jørgensen)	Bol 98		1		AA	130		cool	
<i>Phormospyris stabilis</i> (Goll) <i>scaphipes</i> (Haeckel)	N&M 79		1, 2				SA	cool	subsurface 3,4
<i>Phortidium clevei</i> (Jørgensen)	Bol 98		1, 2		A	92	SA	cool	surface 5
<i>Prunopyle titan</i> Campbell & Clark	Laz 90		1				SA	cool	
<i>Pseudocubus obeliscus</i> Haeckel	Bol 98		1		AA	131		cool	
<i>Saccospyris antarctica</i> Haecker	Bol 98		1, 2		AA	194	SA	cool	
<i>Sethophormis rotula</i> (Haeckel)	Bol 98		1		SA	108		cool	
<i>Siphocampe arachnea</i> (Ehrenberg) group	Nig 77		1, 2		SA	186		cool	
<i>Siphocampe lineata</i> (Ehrenberg) group	Nig 77		1, 2		SA	187		cool	
<i>Spongopyle osculosa</i> Dreyer	N&M 79		1, 2		SA	79	SA	cool	deep 2,4,5
<i>Spongotrochus glacialis</i> Popofsky	Bol 98		1, 2		C	80	SA	cool	surface 2,4,5
<i>Spongotrochus (?) venustum</i> (Bailey)	N&M 79		1, 2					cool	surface 5
<i>Spongurus pylomaticus</i> Riedel	Bol 98		1, 2		AA	82	SA	cool	deep 5
<i>Stylodictya aculeata</i> Jørgensen	Bol 98		1, 2				SA	cool	
<i>Styptosphaera (?) spumacea</i> Haeckel	N&M 79		1, 2		AA	64	SA	cool	
<i>Tricerapsyris antarctica</i> (Haecker)	Bol 98		1		AA	114		cool	

APPENDIX 1

Radiolarian biogeographic affinities and depth preferences for radiolarian taxa from (1) Site 1123 and (2) Site 1124. AA, Antarctic; SA, Subantarctic; TR, Transitional; ST, Subtropical; TT, Tropical zones; C, cosmopolitan. Ref 1, reference to taxon concept: Hk187, Haeckel 1887; Ben 66, Benson 1966; Pet 67, Petrushevskaya 1967; Pet 71, Petrushevskaya 1971b; Pet 72, Petrushevskaya 1972; P&K 72, Petrushevskaya and Kozlova 1972; Nig 77, Nigrini 1977; N&M 79, Nigrini and Moore 1979; N&N 82, Nakaseko and Nishimura 1982; Cau 86, Caulet 1986; C&N 88, Caulet and Nigrini 1988; Laz 90, Lazarus 1990; Tak 91, Takahashi 1991; Bol 98, Boltovskoy 1998. Biogeographic zonations: Mor78, Moore 1978; Bol87, Boltovskoy 1987 (followed by species identification number used in therein); H&N 05, Hollis and Neil 2005. Temp, water temperature affinity. Ref 2, reference to depth zonation: 1, Renz 1976; 2, McMillen and Casey 1978; 3, Kling 1979; 4, Kling and Boltovskoy 1995; 5, Abelmann and Gowing 1997.

ter affinities (Hollis and Neil 2005). In the Atlantic Ocean, the maximum occurrence of living *L. m. maritilis* is found in deep water and within AAIW north of the Polarfrontal Zone, where it is especially abundant in AAIW north of the STF (Abelmann and Gowing 1997).

L. maritilis gr. is most common in Interglacials at both sites, but is more abundant at Site 1123 (text-fig. 4). The warm-water preference of *L. maritilis* gr. is also shown by a negative correlation with $\delta^{18}O$ at Site 1123 ($r = -0.458$). The higher abundance of *L. maritilis* gr. at Site 1123 is probably an artifact of processing; the species group is relatively large and has a robust test.

Phortidium clevei

P. clevei is common in antarctic (Boltovskoy 1987) to subantarctic (Hollis and Neil 2005) waters of the southwest Pacific. It is rare in subtropical waters of the transitional zone (Boltovskoy 1987; Hollis and Neil 2005). *P. clevei* is a shallow dweller occurring with highest densities in the upper 100m of surface waters north and south of the Polarfrontal Zone (Atlantic Sector; Abelmann and Gowing 1997).

At Sites 1123 and 1124 (text-fig. 4), *P. clevei* is generally rare but exceeds 2% in Glacials. A preference for cooler waters is supported by a weak positive correlation with $\delta^{18}O$ at Site 1123 ($r = +0.331$). These features indicate that *P. clevei* is a useful cool-water indicator and it is used here to estimate the influence of shallow, cool SAW north of the STF. The scarcity of *P. clevei* in some Glacial intervals at site 1123 may be a processing artifact as the species is relatively delicate and some individuals are <63 μ m.

Cromyechinus antarctica

In the Pacific Ocean, *Cromyechinus antarctica* is a common faunal element in the antarctic and subantarctic zones south of the STF (Boltovskoy 1987; Hollis and Neil 2005). The species is a deep dweller, living in depths of 400-1000m in the Southern Ocean (Atlantic Sector) where *C. antarctica* represents a major component of Circumpolar Deep Water taxa (Abelmann and Gowing 1997).

At Sites 1123 and 1124, *C. antarctica* is relatively rare (never more than 2%) but increases in abundance in Glacial stages (text-fig. 4). *C. antarctica* is used to detect the influence of deep

Appendix 1 (continued)

TAXA	Ref 1	Comments	Site	Mor78	Bol87	sp. ID	H&N05 Temp	depth	Ref 2
WARM									
<i>Acanthodesmia vinculata</i> (Müller)	Tak 91		1		TT	100	warm	subsurface	1,2
<i>Acanthosphaera dodecastyla</i> Mast	Bol 98		1		ST	17	warm		
<i>Acrosphaera cyrtodon</i> (Haeckel)	Tak 91	Similar to <i>Odontosphaera cyrtodon</i> Haeckel, without curved spines in Hkl 87	1		TT	1	warm		
<i>Acrosphaera lappacea</i> (Haeckel)	N&M 79	As <i>Polysolenia</i>	1		C	2	warm	surface	2
<i>Acrosphaera spinosa</i> (Haeckel)	N&M 79	As <i>Polysolenia</i>	1, 2	TT	TT	4	ST	warm	
<i>Amphirhopalum ypsilon</i> Haeckel	Bol 98		1, 2		TT	68	ST	warm	intermediate 2
<i>Amphispyris reticulata</i> (Ehrenberg)	Bol 98		1		TT	101		warm	
<i>Anomalacantha dentata</i> (Mast)	N&M 79		1, 2		AA	26	ST	warm	
<i>Anthocyrtdium ophirensense</i> (Ehrenberg)	Bol 98		1		ST	173		warm	subsurface 3
<i>Anthocyrtdium zanguebaricum</i> (Ehrenberg)	Bol 98		1		ST	174		warm	
<i>Botryocyrtdis scutum</i> (Harting)	N&M 79		1		ST	191		warm	subsurface 1,2
<i>Carpocanarium papillosum</i> (Ehrenberg) group	N&M 79		1, 2		ST	169	ST	warm	
<i>Clathrocanium coarctatum</i> Ehrenberg	Tak 91		1		ST	119		warm	surface 4
<i>Collosphaera huxleyi</i> Müller	Tak 91		1, 2		C	6	ST	warm	
<i>Collosphaera macropora</i> Popofsky	Bol 98		1		TT	7		warm	
<i>Corocalyptra kruegeri</i> Popofsky	Bol 98		1		TT	137		warm	
<i>Cubotholus</i> spp.	Bol 98		1, 2		TT	99	ST	warm	
<i>Dictyocoryne profunda</i> Ehrenberg	Bol 98		1, 2	TT	TT	69	ST	warm	intermediate 3
<i>Dictyocoryne truncatum</i> (Ehrenberg)	Bol 98		2		TT	70		warm	
<i>Dictyophimus infabricatus</i> Nigrini	Bol 98		1, 2		ST	143		warm	intermediate 3,4
<i>Didymocyrtdis tetrathalamus</i> (Haeckel)	Bol 98		1, 2	C-TT	TT	87	ST	warm	surface 2,3,4
<i>Dipylissa bensoni</i> Dumitrica	Bol 98		1				ST	warm	
<i>Disolenia zanguebarica</i> (Ehrenberg)	N&M 79		1		TT	16		warm	surface 2
<i>Druppatractus irregularis</i> Popofsky	Ben 66		1		C	38	ST	warm	
<i>Euchitonia elegans/furcata</i> (Ehrenberg) group	Bol 98		1, 2	TT	TT	71	ST	warm	surface 1
<i>Eucyrtdium anomalum</i> (Haeckel)	Bol 98		1		TT	146	ST	warm	
<i>Eucyrtdium hexagonatum</i> Haeckel	N&M 79		1		TT	147		warm	surface 1,2
<i>Lamprocyclus maritilis maritilis</i> Haeckel	N&M 79		1, 2		TT	175	ST	warm	deep 5
<i>Lamprocyclus maritilis</i> Haeckel <i>polypora</i> Nigrini	N&M 79		1, 2		C	176	ST	warm	intermediate 3,5
<i>Lamprocyrtis nigriniae</i> (Caulet)	Bol 98		1, 2		ST	177	ST	warm	intermediate 3,4
<i>Lampromitra quadricuspis</i> Haeckel	Bol 98		1, 2		ST	153		warm	intermediate 4

southern-sourced water masses, particularly CDW at the studied sites.

Spongopyle osculosa

In Recent surface sediment samples *Spongopyle osculosa* occurs from the antarctic to subantarctic zone in the Atlantic Sector, with highest abundance in the Polarfrontal Zone (Petrushevskaya 1967; Abelmann and Gowing 1997). Boltovskoy (1987) recorded *S. osculosa* from the tropical to antarctic southwest Pacific but its highest occurrence is within the subantarctic zone and south of the STF offshore eastern New Zealand (Hollis and Neil 2005). Within plankton assemblages in the Atlantic Southern Ocean, Abelmann and Gowing (1997) recorded *S. osculosa* as one of two dominant deep dwellers within AAIW, in water depths of 400-1000 m (the other being *Cycladophora bicornis*; see below). *S. osculosa* is also common in AAIW in the northern subantarctic and subtropical zones (Abelmann and Gowing 1997). *S. osculosa* is recorded in deep water assemblages in the Gulf of Mexico and Caribbean Sea (McMillen and Casey 1978) and in the California Current (Boltovskoy and Riedel 1987). *S. osculosa* is commonly recorded in the vicinity of upwelling regimes, such as the Benguela Current System (Welling et al. 1992; Abelmann and Gowing 1997; Weinheimer 2001). Within the high productivity regime in the equatorial northwest Indian Ocean, Jacot Des Combes et al. (1999) describe *S. osculosa* as part of the thermocline layer assemblage.

S. osculosa exhibits an interesting pattern of occurrence at Site 1123 (text-fig. 4). In the lower part of the record (MIS 15-9), peak abundance is in Interglacials. However, in the late Pleistocene the peaks occur in Glacial stages MIS8, 6, 4 and 2. *S. osculosa* is

generally much less common at Site 1124 and exhibits very slight increases in abundance in Glacial stages MIS6, 4 and 2 (text-fig. 4). *S. osculosa* is thought to indicate the increased influence of AAIW in Glacial stages but in the lower part of Site 1123 it may be associated with enhanced mixing within Interglacials MIS15, 13 and 9. Given this species' robust and relatively large form it is possible that its greater abundance at Site 1123 is partly due to processing differences. However, the increases in Interglacials, which is not evident at Site 1124, signals a stronger influence of deep water mixing at Site 1123.

Cycladophora bicornis

Cycladophora bicornis is a common element of the subantarctic and antarctic Southern Ocean (Lombardi and Boden 1985). In the southwest Pacific, *C. bicornis* occurs in surface sediments north and south of the STF (Boltovskoy 1987), with higher abundance in subantarctic sediments (Hollis and Neil 2005). In the central north Pacific, Gulf of Mexico and Caribbean Sea, *C. bicornis* mainly lives in deep waters of 100-2000m and is most abundant at 200m (Kling 1979, McMillen and Casey 1978). In the Atlantic Sector of the Southern Ocean, *C. bicornis* is a prominent species in the AAIW plankton assemblage of the Polarfrontal Zone where it is most abundant at 100-300m (Abelmann and Gowing 1997). This same AAIW assemblage has also been found in depths between 100 and 500m close to the Namibia Upwelling Regime (Abelmann and Gowing 1997) where intermediate waters upwell along the southwestern African continental margin (Weinheimer 2001).

C. bicornis tends to be most common in Interglacials at Site 1123 (text-fig. 4), an observation supported by the negative correlation

Appendix 1 (continued)

TAXA	Ref 1	Comments	Site	Mor78	Bol87	sp. ID	H&N05	Temp	depth	Ref 2
<i>Larcospira quadrangula</i> Haeckel	Bol 98		1, 2		TT	95	ST	warm	surface	3,4
<i>Lipmanella bombus</i> (Haeckel)	Bol 98		1		TT	154		warm		
<i>Lipmanella dictyoceras</i> (Haeckel)	Bol 98		1, 2		ST	155	ST	warm	surface	4,5
<i>Litharachnium tentorium</i> Haeckel	Bol 98		1, 2		ST	156	ST	warm	subsurface	3,4
<i>Lithopera bacca</i> Ehrenberg	Bol 98		1		ST	157		warm	surface	3
<i>Lithostrobilus hexagonalis</i> Haeckel	Bol 98		1		TT	158		warm	surface	4
<i>Lophophaena hispida</i> (Ehrenberg)	Bol 98		1		ST	123		warm	subsurface	2
<i>Lophospyris pentagona pentagona</i> (Ehrenberg) emend. Goll	Bol 98		1, 2		TT	106		warm		
<i>Octopyle stenozona</i> Haeckel	N&M 79		1, 2		C	91	ST	warm	surface	3
<i>Peromelissa phalacra</i> (Haeckel)	Bol 98		1		ST	129		warm		
<i>Phormospyris stabilis stabilis</i> (Goll)	Bol 98		1		TT	107		warm	subsurface	3
<i>Pterocanium praetextum</i> (Ehrenberg) group	Bol 98		1, 2		TT	160	ST	warm	surface	1,2,4
<i>Pterocorys hertwigii</i> (Haeckel)	Bol 98		1, 2		TT	179		warm	surface	2,4
<i>Pterocorys minythorax</i> (Nigrini)	C&N 88		1		ST	180		warm	surface	4
<i>Pterocorys zancleus</i> (Müller)	Bol 98		1, 2		ST	181		warm	surface	2,4
<i>Saturnalis circularis</i> Haeckel	Bol 98		1		TT	55		warm		
<i>Siphonosphaera martensi</i> Brandt	Bol 98		1		C	10		warm		
<i>Siphonosphaera socialis</i> Haeckel	Tak 91		1		ST	11	ST	warm	surface	4,5
<i>Spirocorys scalaris</i> Haeckel group	Bol 98		1, 2		ST	189		warm	surface	2,4
<i>Spongurus</i> sp. cf. <i>S. elliptica</i> (Ehrenberg)	N&M 79		1		ST	81		warm		
<i>Stylosphaera melpomene</i> Haeckel	Bol 98		1		ST	62		warm		
<i>Tetrapyle octacantha</i> Müller	N&M 79		1, 2	C-TT	C	91	ST	warm	surface	2,3,4,5
<i>Zygocircus productus</i> (Hertwig) group Hertwig	Bol 98		1, 2		ST	115		warm		
TRANSITIONAL										
<i>Actinomma sol</i> Cleve	Bol 98		1, 2		TR	24	TR	transit.	surface	4
<i>Eucyrtidium acuminatum octocolum</i> (Haeckel)	Bol 98		1, 2		TR	149	TR	transit.	intermediate	3
<i>Larcopyle bütschlii</i> Dreyer	Bol 98		1, 2		TR	94	TR	transit.	deep	4
<i>Thecosphaera inermis</i> (Haeckel)	Bol 98		1, 2		TR	65	TR	transit.		
<i>Theocorythium trachelium</i> (Ehrenberg) <i>dianae</i> (Haeckel)	N&M 79		1, 2		TR	182	TR	transit.	surface	3,4,5
<i>Theocorythium trachelium trachelium</i> (Ehrenberg)	N&M 79		1, 2		TR	182	TR	transit.	surface	3,4,5
COSMOPOLITAN										
<i>Acrospira murrayana</i> (Haeckel)	N&M 79	As <i>Polysolenia</i>	1		C	3		cosmop.	surface	2
<i>Actinomma leptoderma leptoderma</i> (Jørgensen)	N&M 79	<i>A. leptodermum</i> (Jørgensen) in N&M 79	1, 2		C	22	C	cosmop.	deep	5
<i>Actinomma medianum</i> Nigrini	N&M 79		1, 2	C	SA	23	C	cosmop.		
<i>Arachnocoallium calvata</i> Petrushevskaya	Pet 71		1		C	117		cosmop.		

with oxygen isotopes ($r = -0.477$). In contrast, *C. bicornis* shows a complex trend at Site 1124, where it has abundance peaks in specific Interglacials (MIS15, 5 and 3) and Glacials (MIS14, 12, 6 and 2) (text-fig. 4). The increased abundance of *C. bicornis* during Interglacials is intriguing given the cool water affinity noted above. Abundance peaks during Interglacials may signal increased deep-water influence or vertical mixing. Abundance peaks in Glacials at Site 1124, including a pronounced acme in MIS12, are consistent with cooling and an increased influence of AAIW at this site. Slightly higher abundance of *C. bicornis* at Site 1124 could be caused by differences in the processing methodology.

Cycladophora davisiana

In the Southern Ocean, *C. davisiana* is most abundant in antarctic waters (Lombardi and Boden 1985). East off New Zealand, the species occurs in surface sediments from north and south of the STF but is significantly more abundant in subantarctic samples (Boltovskoy 1987; Hollis and Neil 2005). In the central north Pacific and in the southern California Current, *C. davisiana* lives in the water column at 50-5000m and has peak abundance in intermediate waters in 100-200m depth (Kling 1979; Kling and Boltovskoy 1995). Nimmergut and Abelmann (2002) reported *C. davisiana* from sediment traps in 200-500m depths in the Okhotsk Sea. In the Antarctic and Polarfrontal Zone of the Atlantic Sector, living *C. davisiana* has been obtained from CDW samples between 400-1000m depth (Abelmann and Gowing 1997). In the western tropical Atlantic and in the Japan Sea, *C. davisiana* has been found in >500m depth (Takahashi and Honjo 1981; Itaki 2003). *C. davisiana* has been described from nearshore upwelling assemblages from the northern California-Current (Welling et al. 1992), from the Benguela Current System

(Weinheimer 2001) and the northwest Indian Ocean (Jacot des Combes et al. 1999). The species is an important stratigraphic tool in carbonate-poor sediments in high latitudes as it is abundant in Glacial times but rare in Interglacials (Hays et al. 1976; Morley and Hays 1979; Abelmann and Gersonde 1988; Morley et al. 1995; Brathauer et al. 2001). Only in the Sea of Okhotsk (Ling 1974; Morley and Hays 1983) and Japan Sea (Itaki 2003), surface sediments contain >20-40% of *C. davisiana*. Hays and Morley (2003) discuss the Sea of Okhotsk as example for Ice Age Ocean conditions.

C. davisiana shows similar trends during the last 600 kyrs at Sites 1123 and 1124 (text-fig. 4). The species tends to be most common in Glacials (text-fig. 4). However, *C. davisiana* has abundance peaks in some Interglacials, especially those in which *C. bicornis* is also common (e.g. MIS15 at Site 1124, MIS9 at Site 1123). As with *C. bicornis*, this suggests that the deep-water influence is enhanced during some Interglacials at both sites. This complex abundance record indicates that, in contrast to high latitudes, *C. davisiana* is not a reliable guide for Glacial conditions in mid-latitudes. The higher abundance of this small species at Site 1124 could be due to processing differences between Sites 1123 and 1124.

Radiolarian assemblage variation: Glacial/Interglacial comparisons

Interglacial assemblages in 13 samples at Site 1123 are relatively diverse and are dominated by three undifferentiated spumellarian families (litheliids, spongodiscids, actinommids) (text-fig. 5a). *Larcopyle bütschlii* and *Theocorythium trachelium dianae* are the only transitional taxa to exceed 1% of the assemblage within Interglacials. *Tetrapyle octacantha* gr. is the only com-

Appendix 1 (continued)

TAXA	Ref 1	Comments	Site	Mor78	Bol87	sp. ID	H&N05	Temp	depth	Ref 2
<i>Axoprunum stauraxonium</i> Haeckel	N&M 79		1, 2		C	28	C	cosmop.		
<i>Botryopyle dictyocephalus</i> Haeckel	Bol 98		1		C	192		cosmop.		
<i>Botryostrobos auritus/australis</i> (Ehrenberg)	Bol 98		1, 2		C	185	C	cosmop. intermediate	3,4	
<i>Carpocanistrum</i> spp.	N&M 79		1, 2		ST	170,171	C	cosmop. intermediate	4	
<i>Ceratocyrtis histricosus</i> (Jørgensen)	Bol 98	<i>Helotholus histricosus</i> Jørgensen in Bol 98	1, 2		AA	121	C	cosmop. surface	4	
<i>Circodiscus microporus</i> (Stöhr)	P&K 72		1, 2				C	cosmop.		
<i>Cladoscenium ancoratum</i> Haeckel	Tak 91		1		C	118		cosmop.		
<i>Cornutella profunda</i> Ehrenberg	Bol 98		1, 2		SA	135	C	cosmop. intermediate	4	
<i>Corocalyptra cervus</i> (Ehrenberg)	Bol 98		1, 2		C		C	cosmop. intermediate	1,5	
<i>Corocalyptra columba</i> (Haeckel)	Bol 98		1		C	136		cosmop. deep	4	
<i>Cyrtopera laguncula</i> Haeckel	Bol 98		1, 2		C	139		cosmop. intermediate	3,4	
<i>Dictyophimus hirundo</i> (Haeckel)	Bol 98		1, 2		C	142	C	cosmop.		
<i>Eucyrtidium acuminatum acuminatum</i> (Ehrenberg)	N&M 79		1, 2		C	145	C	cosmop. surface	4	
<i>Eucyrtidium annulatum</i> (Popofsky)	Ben 66		1		C	151		cosmop.		
<i>Eucyrtidium hexastichum</i> (Haeckel)	Bol 98		1		C	148		cosmop. surface	4,5	
<i>Eucyrtidium teuscheri</i> (Haeckel)	Cau 86		1, 2				C	cosmop.		
<i>Gondwanaria dogieli</i> (Petrushevskaya)	N&N 82		1, 2				C	cosmop. deep	4	
<i>Haliometta miocenica</i> (Campbell & Clark)	N&N 82		1, 2				C	cosmop.		
<i>Heliodiscus asteriscus</i> Haeckel	Bol 98		1, 2		C	90	C	cosmop. surface	2,3	
<i>Hexacantium armatum/hostile</i> Cleve group	N&M 79	<i>H. enthacanthum</i> Jørgensen in N&M 79	1, 2		C	45,46	C	cosmop.		
<i>Hexacantium laevigatum</i> Haeckel	N&M 79		1		TT	49	C	cosmop.		
<i>Lithelius minor</i> Jørgensen group	Bol 98		1, 2	C			C	cosmop.		
<i>Phormostichoartus corbula</i> (Harting)	N&M 79		1		C	188		cosmop. subsurface	3	
<i>Pseudodictyophimus gracilipes</i> (Bailey)	Tak 91		1, 2		C	141	C	cosmop. intermediate	3,4,5	
<i>Pterocanium trilobum</i> (Haeckel)	Bol 98		1, 2		C	161	C	cosmop. surface	4	
<i>Pterocorys clausus</i> (Popofsky)	C&N 88		1, 2		SA	178	C	cosmop. subsurface	3,4	
<i>Pylolella armata</i> Haeckel group	Bol 98		1, 2		TT	93	C	cosmop. surface	2	
<i>Pylolella octopyle</i> Haeckel	Bol 98		1, 2		TT	98	C	cosmop.		
<i>Sethocomus (?) tabulatus</i> (Ehrenberg)	Pet 67		1, 2		C	162		cosmop.		
<i>Spongocore puella</i> Haeckel	N&M 79		1, 2		C	76	C	cosmop. intermediate	3	
<i>Spongodiscus resurgens</i> Ehrenberg	Bol 98		1, 2		C	77	C	cosmop. subsurface	3	
<i>Spongurus ? sp.</i>	N&M 79		1, 2		C	83	C	cosmop. deep	4, 5	
<i>Stichopilium bicornis</i> Haeckel	N&M 79		1		C	164		cosmop. subsurface	3	
<i>Stylatractus</i> spp. gr.	Bol 98		1, 2		C	60,61	C	cosmop.		

mon warm-water taxon (text-fig. 5a). Three cool-water taxa are abundant during Interglacials, including *Cycladophora bicornis* as noted above. Glacial assemblages in 12 samples are slightly less diverse (22 vs 24 taxa with an average abundance of >1% of the assemblage) but are similarly dominated by undifferentiated spumellarians (text-fig. 5b). A significant difference is the high abundance of the cool-water genus *Cenosphaera* (>10%). The warm-water *T. octacantha* gr. remains common but much less so than in Interglacials.

Because undifferentiated spumellarians are such a dominating feature of Glacial assemblages, only two definitively cool-water species occur at >1% in Glacial assemblages: *Spongopyle osculosa* and *Cycladophora davisiana*.

Assemblages from Site 1124 are generally more diverse than those from Site 1123, have high Equitability and have reduced dominance of undifferentiated spumellarians (text-fig. 5c, d). Interglacial assemblages in 39 samples are dominated by cosmopolitan taxa but the warm-water *T. octacantha* gr. is very common, exceeding 5% of the assemblage (text-fig. 5c). *Dictyocoryne profunda* and *Lophospyris pentagona pentagona* are two other common warm-water species. As discussed in the previous section, two subantarctic species, *C. davisiana* and *C. bicornis* are also relatively common in Interglacials. Glacial assemblages in 33 samples for Site 1124 are in general respects quite similar to Interglacial assemblages (text-fig. 5d). The main difference is the greater abundances of cool-water species, especially *C. davisiana*. In contrast to Site 1123 *L. bütschlii* and *T. t. dianae* are common transitional species within Interglacials and Glacials at Site 1124.

An exceptional species assemblage occurs in uppermost MIS8 at Site 1123 (1123B-2H-6, 80-82cm). The sample has an Interglacial character in terms of high abundance and diversity, as discussed above. Also, warm-water taxa (e.g. *Acrosphaera spinosa*, *Didymocyrtis tetrathalamus*) are much more common than cool-water taxa (e.g. *Cenosphaera cristata*, *Cycladophora bicornis*, *Botryostrobos aquilonaris*; Appendix 1). The sample may represent a warm anomaly within MIS8 or it might be out of place within the sedimentary succession. Unfortunately, no records for MIS8 are available for Site 1124 due to a hiatus.

Radiolarian paleotemperature indicators

Local information (Moore 1978; Boltovskoy 1987; Hollis and Neil 2005) on the modern biogeographic distribution of species and species groups encountered in this study has been used to assign 93 taxa to one of three categories: warm-water (tropical-subtropical), transitional, and cool-water (subantarctic-antarctic) (text-fig. 6; Appendix 1). As described earlier, the ratio of warm-water to cool-water species defines a new paleotemperature indicator: the Subtropical Index (ST index).

In the spumellarian-dominated record at Site 1123, paleotemperature indicator species rarely exceed 15% of the total fauna. Cool- and warm-water taxa have similar mean values (~6%) and, as expected, tend to vary antithetically in relation to oxygen isotope-defined climate cycles, especially in the upper part of the record (text-fig. 6). An exception to this pattern occurs in the lower part of the record where cool-water indicators show significant increases in Interglacials, notably MIS15, 13, 11 and 9. This is largely due to increases in deep-water indicators (*Cycladophora* spp., *S. osculosa*) and, as noted above, suggests increased deep-water influence during these middle Pleistocene Interglacials. The decline in cool-water taxa in uppermost parts

Appendix 1 (continued)

TAXA	Ref 1	Comments	Site	Mor78	Bol87	sp. ID	H&N05	Temp	depth	Ref 2
<i>Stylochlamidium</i> spp.	N&N 82		1, 2		C	84	C	cosmop.		
<i>Stylodictya validispina</i> Jørgensen	N&M 79		1, 2	C	C	85	C	cosmop. surface		2
<i>Theocorys veneris</i> Haeckel	Tak 91		1, 2		C	167		cosmop. subsurface		3, 4
<i>Theopilium tricostatum</i> (Haeckel)	Bol 98		1		C	168		cosmop. subsurface		2, 4

of Glacials MIS12 and 10 reflects the dominance of undifferentiated spumellarians, which cannot be assigned to biogeographic categories (see also text-fig. 5). Although the abundant genus *Cenosphaera* is dominated by cool-water species in this region, the presence of some warm-water elements precludes its use as a paleotemperature indicator (text-fig. 5). Transitional taxa make up ~3% of the total fauna on average and generally follow the pattern of warm-water taxa, increasing in Interglacials and decreasing in Glacials (text-fig. 6).

The high resolution record at Site 1124 shows well-defined antithetic variation in the abundance of paleotemperature indicator species in relation to climate cycles (text-fig. 6). On average, paleotemperature indicator species comprise >20% of the total fauna through the record. In contrast to the record at Site 1123, warm-water elements tend to be more common at Site 1124 and are rarely less than 10% (text-fig. 6). Transitional taxa average ~5% at Site 1124 and do not exhibit a clear trend in relation to climate cycles, with abundance peaks occurring in Glacials as well as Interglacials (text-fig. 6).

The Subtropical (ST) Index provides a useful summary of the trends discussed above and serves to accentuate the paleotemperature signal preserved in assemblages from both sites (text-fig. 6). Despite processing differences, the ST Index offsets between the two sites are consistent with the general biogeographic character of the assemblages, as discussed above, with the ST Index being generally higher at Site 1124, especially during Interglacials. The ST Index indicates that the warmest Interglacials are MIS11 (Site 1123 only), MIS7 and MIS5 and the coolest Glacials are MIS12 (at Site 1123), MIS6 and MIS2. Regarding Glacials at Site 1123 it has to be considered that MIS 12 is very depleted in paleotemperature indicator species and MIS2 is recorded by a single sample.

Local temperature changes throughout G-I climate cycles have been documented in local marine records using e. g. foraminifera and alkenones (Crundwell et al. in press; Pahnke and Sachs) which are in covariance with local (Hall et al. 2001, 2002) and global (Shackleton and Hall 1989) benthic foraminifera oxygen isotope records. Use of the radiolarian ST Index as a paleotemperature proxy is supported by a strong negative correlation of -0.728 with $\delta^{18}O$ at Site 1123 (Appendix 2b). However, it is interesting to note that while the percentage of warm-water indicators also shows a significant negative correlation with $\delta^{18}O$, there is no significant correlation with cool-water indicators. This reinforces the observation that temperature is not the sole influence on the abundance of cool-water taxa at Site 1123. This observation is reinforced by the absence of a correlation between warm- and cool-water indicators at Site 1123 (Appendices 2a, b), which contrasts with the strong negative correlation (-0.633) between these indicator groups at Site 1124 (Appendix 2c). Another important difference between the two sites in terms of covariance patterns is the significant positive correlation between diversity and both warm and cool paleotemperature indicators at Site 1123. This is not observed at Site 1124 and implies that the presence of identifiable paleotemperature indicators at Site 1123 may be a function of preservation. As preservation improves, the unexpected out-

come of the resulting diversity increase appears to be increases in the abundance of both warm- and cool-water indicator taxa. That no such correlation exists at Site 1124 is likely due to consistent good preservation through the late Pleistocene succession.

Radiolarian paleodepth indicators

It is difficult to differentiate paleodepth signals from paleotemperature signals in radiolarian assemblages because most of the species that inhabit surface or near-surface watermasses in high latitudes also inhabit deep watermasses at lower latitudes. In the preceding section, the paleotemperature records for both sites are based on variations in abundance of paleotemperature indicators from a range of depth zones. In this section, we subdivide the taxa according to depth preferences in order to determine if faunal changes help to identify changes in watermass structure at the two sites.

Variation in the abundance of shallow-dwelling taxa can be used to identify changes in the influence of surface watermasses north of the STF (text-fig. 7). Of the 29 shallow-dwelling taxa at Sites 1123 and 1124, warm-water elements are the most common and most diverse (23 warm-water and 6 cool-water taxa; Appendix 1). Especially at Site 1124, the ratio of warm-water taxa over cool-water taxa within shallow waters is almost twice as high as at Site 1123 which is partly due to differences in the processing methods. The abundance of warm-water, shallow dwelling taxa essentially mirrors that of the total warm-water cohort at both sites (text-fig. 6), peaking in Interglacials and decreasing through Glacials. In contrast, the cool-water shallow dwelling taxa differ from the total cool-water cohort in two important respects. Abundance peaks are intensified in a few Glacials, especially MIS12 at both sites and in uppermost MIS14 and MIS6 at Site 1124. This implies intensification of SAW flow at these times. Secondly, abundance peaks are muted in the Glacials in the late Middle to early Late Pleistocene at Site 1123, especially in MIS 10 and 6. This suggests relatively weak influence of SAW over Site 1123 at this time.

To determine the influence of intermediate water masses (AAIW) and deep southern-sourced currents (e.g. DWBC) at Sites 1123 and 1124 abundance of cool-water, deep-dwelling radiolarians has been investigated. Radiolarians living in depths >150m and have peak abundance at 200m water depths include *Cycladophora bicornis*, *Spongopyle osculosa*, *Peripyramis circumtexta*, *Androcyclas gamphonycha* and *Botryostrobilus aquilonaris* (Appendix 1) and are inferred to be AAIW indicators (text-fig. 7). Deeper dwelling *Cromyechinus antarctica*, *Spongurus* ? sp. and *Spongurus pylomaticus* inhabit depths of >300m within CDW of the Southern Ocean (Abelmann and Gowing 1997). The influence of these southern-sourced, deep water masses is strongest in Glacials in the upper part of Site 1123 (MIS8 to MIS2) and throughout the interval examined at Site 1124 (text-fig. 7). In the lower part of Site 1123, this deep-water influence is strongest in the Interglacials (MIS15 to MIS9). The high abundance of deep-dwelling taxa in these Interglacials is a possible indication for enhanced vertical mixing. In MIS12 and 10, the weakness of a southern-sourced water mass signal is an artefact of the scarcity of paleoenvironmental indicators in spu-

Appendix 2 (a) Site 1123 (0-1.2 Ma)

	$\delta^{18}\text{O}$	rads/g	# taxa	α	H(S)	E	%SA	%ST	ST Index	%TR	shallow STW	shallow SAW	comb. CDW+AAIW	CDW comp.	AAIW comp.
$\delta^{18}\text{O}$	1.000	-0.032	-0.294	-0.255	-0.337	-0.002	0.242	-0.584	-0.557	-0.021	-0.501	0.306	0.110	0.207	0.069
rads/g		1.000	0.586	0.624	0.470	0.321	0.243	0.337	-0.067	0.014	0.390	0.223	0.239	0.317	0.189
# taxa			1.000	(0.968)	(0.944)	(0.250)	0.493	0.718	0.017	-0.294	0.696	0.234	0.518	0.339	0.514
α				1.000	(0.932)	(0.330)	0.522	0.664	-0.053	-0.272	0.653	0.273	0.538	0.399	0.520
H(S)					1.000	(0.331)	0.528	0.722	0.023	-0.301	0.671	0.249	0.554	0.319	0.562
E						1.000	0.298	0.200	-0.248	0.271	0.147	0.178	0.331	0.332	0.294
%SA							1.000	0.118	(-0.572)	-0.137	0.172	(0.593)	(0.917)	(0.598)	(0.910)
%ST								1.000	(0.497)	-0.220	(0.885)	-0.017	0.221	0.087	0.236
ST Index									1.000	-0.078	(0.354)	(-0.403)	(-0.431)	(-0.363)	(-0.404)
%TR										1.000	-0.241	-0.048	-0.173	0.069	-0.226
shallow STW											1.000	0.125	0.221	0.024	0.256
shallow SAW												1.000	0.422	0.291	0.415
CDW+AAIW													1.000	(0.704)	(0.977)
CDW comp.														1.000	0.538
AAIW comp.															1.000

Appendix 2 (b) Site 1123 (0-0.6 Ma)

	$\delta^{18}\text{O}$	rads/g	# taxa	α	H(S)	E	%SA	%ST	ST Index	%TR	shallow STW	shallow SAW	comb. CDW+AAIW	CDW comp.	AAIW comp.
$\delta^{18}\text{O}$	1.000	-0.127	-0.481	-0.490	-0.525	-0.083	0.167	-0.680	-0.728	0.206	-0.642	0.362	0.051	0.163	0.017
rads/g		1.000	0.639	0.651	0.475	0.293	0.089	0.422	0.173	0.019	0.470	0.073	0.109	0.235	0.068
# taxa			1.000	(0.981)	(0.960)	(0.465)	0.466	0.820	0.351	-0.159	0.766	0.084	0.507	0.396	0.506
α				1.000	(0.937)	(0.473)	0.443	0.809	0.349	-0.168	0.743	0.080	0.494	0.439	0.478
H(S)					1.000	(0.466)	0.508	0.818	0.339	-0.121	0.737	0.114	0.538	0.427	0.535
E						1.000	0.201	0.367	0.010	0.115	0.255	-0.044	0.296	0.369	0.257
%SA							1.000	0.187	(-0.422)	-0.165	0.154	(0.577)	(0.925)	(0.710)	(0.925)
%ST								1.000	(0.735)	-0.233	(0.946)	-0.079	0.269	0.149	0.285
ST Index									1.000	-0.269	(0.711)	(-0.367)	(-0.315)	(-0.276)	(-0.276)
%TR										1.000	-0.260	0.068	-0.318	-0.221	-0.325
shallow STW											1.000	-0.002	0.200	0.035	0.233
shallow SAW												1.000	0.378	0.247	0.390
CDW+AAIW													1.000	(0.817)	(0.987)
CDW comp.														1.000	0.715
AAIW comp.															1.000

Appendix 2 (c) Site 1124 (0-0.6 Ma)

	rads/g	# taxa	α	H(S)	E	%SA	%ST	ST Index	%TR	shallow STW	shallow SAW	comb. CDW+AAIW	CDW comp.	AAIW comp.
rads/g	1.000	0.452	0.383	0.428	0.216	-0.202	0.097	0.143	-0.127	0.071	-0.251	-0.195	-0.227	-0.136
# taxa		1.000	(0.851)	(0.876)	(0.248)	-0.146	0.211	0.153	-0.210	0.262	-0.112	-0.170	-0.183	-0.129
α			1.000	(0.851)	(0.416)	-0.157	0.227	0.129	-0.231	0.205	-0.132	-0.156	-0.184	-0.108
H(S)				1.000	(0.677)	-0.088	0.125	0.095	-0.203	0.129	-0.044	-0.089	-0.096	-0.067
E					1.000	-0.006	-0.039	-0.004	-0.060	-0.121	0.039	0.040	0.054	0.023
%SA						1.000	-0.633	(-0.767)	0.142	-0.457	(0.792)	(0.910)	(0.774)	(0.803)
%ST							1.000	(0.750)	-0.191	(0.795)	-0.571	-0.535	-0.668	-0.349
ST Index								1.000	-0.145	(0.514)	(-0.552)	(-0.716)	(-0.680)	(-0.590)
%TR									1.000	-0.244	0.241	0.152	0.312	0.028
shallow STW										1.000	-0.387	-0.469	-0.548	-0.328
shallow SAW											1.000	0.609	0.685	0.441
CDW+AAIW												1.000	(0.771)	(0.929)
CDW comp.													1.000	0.481
AAIW comp.														1.000

APPENDIX 2

Linear correlation coefficients for radiolarian assemblage characteristics (and $\delta^{18}\text{O}$ for Site 1123; from Hall et al. 2001) for (a) the entire 1.2 Myr record examined at ODP Site 1123 (N = 55; $r \geq 0.267$ is significant at P = 0.05), (b) the last 0.6 Myrs at Site 1123 (N = 25; $r \geq 0.396$ is significant at P = 0.05), and (c) the 0.6 Myr record at Site 1124 (N = 72; $r \geq 0.238$ is significant at P = 0.05). Significant correlations are in bold type. Correlations between non-independent radiolarian parameters are in brackets. %SA, abundance of cool-water taxa; %ST, abundance of warm-water taxa; %TR, abundance of transitional taxa. Other symbols as for text-figs. 2, 7.

mellarian-dominated assemblages at Site 1123 (text-fig. 7). From MIS7, a switch in the deep ocean regime seems to occur which strengthens the influence of deep, cool southern-sourced waters within Glacials. Over the same interval, the CDW signal, that is associated with DWBC flow, is no longer evident in Interglacials. At both Sites, the strongest episode of cool deep-water influence is within MIS2 where deep-dwelling radiolarians exceed 10% of the assemblage (text-fig. 7).

DISCUSSION

Interglacial assemblages

Radiolarian assemblages at ODP Site 1123, and, in particular at Site 1124, are abundant and diverse during Interglacials (text-fig. 2). This is also seen in modern radiolarian assemblages north of the STF (Hollis and Neil 2005) and is consistent with a micronutrient-rich, highly-productive STW inflow (Boyd et al. 2004). At

Site 1124, the strong influence of northern-sourced ECC flow is evident from an abundance of warm-water species. Radiolarian assemblages at Site 1123 are less abundant and diverse during Interglacials than at Site 1124. At Site 1123, we infer advection of micronutrient-poor SAW (Boyd et al. 2004) across or around the eastern edge of Chatham Rise (Chiswell and Sutton 1998; Chiswell 2001). In the area off the eastern rise, the STF-controlling Southland Current (SC) and the ECC are less constrained by the deepening rise (2000m; Chiswell 2001), allowing widening of the front up to 400km. Satellite-derived images of sea surface temperature (SST) in the eastern offshore New Zealand region show both intrusions of SAW north into STW and reverse out-breaks over the STF (Chiswell 2001). SST oscillations, at scales ranging from tens to hundreds of kilometers, however, do not affect the steep thermohaline feature of the STF (Chiswell 2001).

Spumellarian-dominated assemblages at Sites 1123 and 1124 have increased abundance of warm-water families, namely collosphaerids, coccodiscids, tholoniids and nassellarian pterocoryids within Interglacials (text-fig. 3), which are the radiolarian families that typify subtropical and tropical watermasses in the southwest Pacific (Boltovskoy 1987). The high-resolution record at Site 1124 reveals a rapid increase of warm-water taxa at glacial terminations (text-fig. 6). Radiolarian assemblages indicate that warmest conditions and strongest influence of shallow, warm STW occurred at the onset of Interglacials within MIS11 (Site 1123), MIS7 (Sites 1123, 1124) and MIS5 (Sites 1123, 1124) (text-fig. 7). Sea-surface temperature (SST) reconstructions at Site 1123, based on planktic foraminifera, suggest warmest mean annual SSTs of ~19°C at the onset of MIS11, 9, 7, and, SSTs of ~18°C in initial MIS5 (Crundwell et al. in press). The abrupt increase in tropical and subtropical elements at the onset of Interglacials is consistent with sedimentary evidence for a strengthening of south-flowing subtropical waters of the ECC (e.g. Carter et al. 1999b; Carter 2001; Nelson et al. 2000). Carter et al. (2002) noted that the main driving force of the ECC, namely the Tasman Front/East Australian Current, migrated southward to its present position at ~32°S after the Last Glacial Maximum (LGM), which is assumed to allow the current to pass through a major gap in Norfolk Ridge, thus enforcing the downstream ECC. This southward migration of the front presumably occurred in all Interglacials and caused increased abundance of warm-water radiolarians. An increased abundance of deep-dwelling taxa in some Interglacials at Site 1123 (text-fig. 7) is considered to indicate enhanced vertical mixing and is discussed further below.

Glacial assemblages

Reduced abundance and diversity characterize Glacials, especially at Site 1123. This is assumed to be due to the weakened flow of STW. During the LGM, the Tasman Front/East Australian Current was positioned at ~26°S (Martinez 1994) and ~600km north of its present position (Carter 2001). Thus, the southward flow of STW was thought to be weakened and partly deflected by Norfolk Ridge (Carter et al. 2002). Concurrent northward incursions of SAW across, and around the deep eastern edge of Chatham Rise (Chiswell and Sutton 1998; Chiswell 2001) would cause particularly low abundance and diversity at Site 1123 (text-fig. 2). Crundwell et al. (in press) also suggest a northward shift of the STF, and migration of SAW over the position of Site 1123 during Glacials. Expansion of ice caps is believed to have intensified temperature gradients, the flow of westerly winds, circumpolar currents and the associated DWBC flow resulting in the northward migration of ocean fronts in the Southern Ocean (Carter 2001; Hall et al. 2001; 2002). Because of the topographic restriction, northward oscillation of the STF

is unlikely over the shallow, central Chatham Rise (Heath 1985; Fenner et al. 1992; Nelson et al. 1993; Carter 2001; Chiswell 2002; Sikes et al. 2002).

Glacial radiolarian assemblages at Sites 1123 and 1124 are dominated by spongodiscids and litheliids and have increased abundance of carpocaniids, cannobotryids, artostrobiids, as well as cool-water actinommids, pyloniids and theoperids (text-fig. 3). Radiolarian paleotemperature and depth indicators also suggest reduced supply of shallow STW to the eastern New Zealand area, and, at the same time, increased influence of cool SAW during Glacials (text-fig. 7). Lowest ST Index values indicate coolest conditions in MIS12 (Site 1123), MIS6 (Sites 1123, 1124), MIS4 (Site 1123) and MIS2 (Sites 1123, 1124; text-fig. 6). Oxygen isotope records at Site 1123 suggest coolest Glacials in MIS 12 and 2 (Hall et al. 2001; 2002); MIS12 is considered to be the coldest Glacial in the past 500,000 years (Howard 1997). Derived from planktic foraminiferal assemblages, Crundwell et al. (in press) propose SSTs of ~10°C (MIS6), ~11°C (MIS12, 4) and ~12°C (MIS2) at Site 1123.

Sedimentological and stable isotope data indicate that the intensity of DWBC flow increases during Glacials and that the flow has shown a progressive increase in successive Glacial stages from ~4 Ma (Hall et al. 2001). This is broadly consistent with the radiolarian record, although the low resolution of the Site 1123 record and the hiatus in the critical interval at Site 1124 make confident interpretation of the deep-water signal difficult. Based on the abundance of deep-water indicators, deep water influence is strongest in the last three Glacial stages (MIS6, 4 and 2) and peaks in MIS2 (text-fig. 7). Prior to MIS7 (~0.25 Ma), there is little indication that deep-water influence is significantly stronger in Glacials than in Interglacial with peaks in deep-water indicators occurring rather randomly through the record. There is little evidence to support the suggestion by Joseph et al. (2004) that DWBC flow became progressively weaker through the Quaternary at Site 1124 due to the current migrating away from the location.

Vertical mixing during Interglacials

Peaks in the abundance of deep-dwelling radiolarian species, such as *C. bicornis* and *S. osculosa*, have been used to identify episodes of high export productivity and enhanced vertical mixing within upwelling areas (Welling et al. 1992; Abelmann and Gowing 1997; Jacot Des Combes et al. 1999; Weinheimer 2001; text-fig.6). As these are also cool-water species, increases in their abundance during Glacial stages at Sites 1123 and 1124 are an expected feature of cooler-water assemblages. However, significant peaks in Interglacials are possibly caused by deep-water indicators; local changes in oceanographic conditions may have promoted vertical mixing. *C. bicornis* and *S. osculosa* have abundance peaks in Interglacials (MIS 15, 13 and 9) in the lower part of the Site 1123 record and also exhibit small increases in MIS15 and 13 at Site 1124 (text-fig. 4). In the upper part of the two records, peak abundances for these two species are largely restricted to Glacial stages, apart from peaks for *C. bicornis* in MIS5 and MIS3 (text-fig. 4). This suggests that enhanced vertical mixing was primarily a feature of Interglacials prior to ~0.25 Ma. However, there is no evidence from the radiolarian faunas to suggest that this resulted in increased export productivity. Indeed, radiolarian abundance and diversity increase at Site 1123 from the base of Interglacial MIS9 and both parameters are stable through this interval at Site 1124 (text-fig. 2). Rather than a paleoproductivity signal, the abundance peak for these two deep-water species in middle Pleistocene Interglacials (MIS15-9) suggests that a compositional difference in the deep water

bathing the two sites, especially Site 1123, occurred at ~2.5 Ma. The cause for this shift is uncertain but it may be related to an overall increase in DWBC flow that begins at ~0.45 Ma (Hall et al. 2001).

SUMMARY AND CONCLUSIONS

Variations in radiolarian abundance, diversity and in the abundance of paleotemperature and paleodepth indicators at Sites 1123 and 1124 during G-I cycles provide useful guides to changes in oceanographic conditions offshore eastern New Zealand during the last 600,000 years.

Radiolarian assemblages north of the STF are abundant and diverse, reflecting nutrient-rich, productive conditions under STW inflow, particularly at Site 1124. A radiolarian paleotemperature proxy, the Subtropical (ST) Index indicates warmest climatic conditions occurred during Interglacial Stages MIS 11, 7 and 5. Diverse Interglacial faunas comprise mostly warm-water and shallow-dwelling taxa that reflect a strong inflow of the subtropical ECC, probably caused by southward shift of the Tasman Front/East Australian Current. Abundance peaks of deep-dwelling taxa within Interglacials between 0.6 and 0.25 Ma (MIS15-9) indicate enhanced vertical mixing but radiolarian assemblages do not indicate that this was associated with high productivity: radiolarian abundance and diversity are highest in the latest Quaternary Interglacials. The ST Index indicates that coolest climatic conditions occurred in MIS 12, 6 and 2. Paleotemperature and paleodepth indicators indicated reduced subtropical inflow during Glacials, particularly at Site 1123. Radiolarian assemblages suggest that the STF may have migrated over Site 1123 during the coolest Glacial episodes, probably due to the strengthening of deep, southern-sourced currents.

ACKNOWLEDGMENTS

VL acknowledges the German Academic Exchange Service (Deutscher Akademischer Austausch Dienst, DAAD); VL and HW thank the German Research Foundation (Deutsche Forschungsgemeinschaft, DFG) and the University of Bremen; VL and CH are grateful for support from the Foundation for Research, Science and Technology through the GNS Global Change Through Time Program. The authors thank the Ocean Drilling Program for providing samples from Sites 1123 and 1124. We are grateful to Ian Hall for providing stable isotope and color reflectance data for Sites 1123 and 1124, and for the revised age model from Site 1123. The authors thank Martin P. Crundwell, George H. Scott and Karin A. F. Zonneveld for helpful discussions and critical review of this work. The thorough analysis and perceptive comments on the manuscript by David B. Lazarus and Jane K. L. Dolven were much appreciated.

REFERENCES

ABELMANN, A., 1988. Freeze-drying simplifies the preparation of microfossils. *Micropaleontology*, 34(4): 361.

ABELMANN, A. and GERSONDE, R., 1988. *Cycladophora davisiana* stratigraphy in Plio-Pleistocene cores from the Antarctic Ocean (Atlantic Sector). *Micropaleontology*, 34(3): 268-276.

ABELMANN, A. and GOWING, M.M., 1997. Spatial distribution pattern of living polycystine radiolarian taxa - baseline study for paleoenvironmental reconstructions in the Southern Ocean (Atlantic Sector). *Marine Micropaleontology*, 30: 3-28.

ABELMANN, A., BRATHAUER, U., GERSONDE, R., SIEGER, R. AND ZIELINSKI, U., 1999. Radiolarian-based transfer function for the estimation of sea surface temperatures in the Southern Ocean (Atlantic Sector). *Paleoceanography*, 14(3): 410-421.

AITA, Y. and SUZUKI, A., 2003. Leg 181: Southwest Pacific Gateways: Sediment drift and deep water fluctuation off Eastern New Zealand. *Monthly Chikyu Special Volume: Deep Sea and a new Earth Biological Science*, Kaiyo-Shuppan, 40: 1-5.

BENSON, R.N., 1966. "Recent Radiolaria from the Gulf of California". Ph.D. thesis, University of Minnesota, Minnesota, 577 pp.

BEVINGTON, P.R. and ROBINSON, D.K., 1991. *Data reduction and Error Analysis for the Physical Sciences*. London, McGraw-Hill Higher Education, Inc.: 328 pp.

BOLTOVSKOY, D., 1987. Sedimentary record of radiolarian biogeography in the equatorial to antarctic western Pacific Ocean. *Micropaleontology*, 33(3): 267-281.

———, 1998. Classification and distribution of South Atlantic recent polycystine Radiolaria. *Paleontologica Electronica*, 1(2): 1-116. [http://www.paleo-electronica.org/1998_2/boltovskoy/issue2.htm]

BOLTOVSKOY, D. and RIEDEL, W.R., 1980. Polycystine Radiolaria from the southwestern Atlantic Ocean plankton. *Revista Espanola de Micropaleontologia*, 12(1): 99-146.

BOLTOVSKOY, D. and JANKILEVICH, S.S., 1985. Radiolarian distribution in East equatorial Pacific plankton. *Oceanologica Acta*, 8(1): 101-123.

BOYD, P.W., MCTAINSH, G., SHERLOCK, V., RICHARDSON, K., NICHOL, S., ELLWOOD, M. and FREW, R., 2004. Episodic enhancement of phytoplankton stocks in New Zealand subantarctic waters: contribution of atmospheric and oceanic iron supply. *Global Biogeochemical Cycles*, 18: 1029, doi:10.1029/2002GB002020.

BRATHAUER, U., ABELMANN, A., GERSONDE, R., NIEBLER, H.-S., and FÜTTERER, D.K., 2001. Calibration of *Cycladophora davisiana* events versus oxygen isotope stratigraphy in the subantarctic Atlantic Ocean - a stratigraphic tool for carbonate-poor Quaternary sediments. *Marine Geology*, 175: 167-181.

CARTER, L., 2001. Currents of change: the ocean flow in a changing world. *Water and Atmosphere*, 9(4): 15-17. NIWA online publications [<http://www.niwascience.co.nz>].

CARTER, R.M., CARTER, L., MCCAVE, N., and THE LEG 181 SHIPBOARD SCIENTIFIC PARTY, 1999a. The DWBC sediment drift record from Leg 181: drilling in the Pacific gateway for the global thermohaline circulation. *JOIDES Journal*, 25(1): 8-13.

CARTER, R.M., MCCAVE, I.N., RICHTER, C., CARTER, L., AND THE LEG 181 SHIPBOARD SCIENTIFIC PARTY, 1999b. *Proceedings of the Ocean Drilling Program, Initial Reports, Southwest Pacific Gateways, Volume 181*. College Station, TX: Ocean Drilling Program, [CD-ROM].

CAULET, J.P., 1986. Radiolarians from the Southwest Pacific. In: Kennett, J.P., Von Der Borch, C.C., et al., Eds. *Initial Reports of the Deep Sea Drilling Project*, Volume 90, Washington DC: US Government Printing Office, 90: 835-861.

CAULET, J.P. and NIGRINI, C., 1988. The genus *Pterocorys* [Radiolaria] from the tropical late Neogene of the Indian and Pacific Oceans. *Micropaleontology*, 34(3): 217-235.

- CASEY, R.E., 1971. Radiolarians as indicators of past and present water-masses. In: Funnel, B.M. and Riedel, W.R., Eds., *The Micropalaeontology of Oceans*. London: Cambridge University Press, 331-341.
- CHISWELL, S.M., 1994. Variability in sea surface temperature around New Zealand from AVHRR images. *New Zealand Journal of Marine and Freshwater Research*, 28: 179-192.
- , 2000. The Wairarapa Coastal Current. *New Zealand Journal of Marine and Freshwater Research*, 34: 303-315.
- , 2001. Eddy energetics in the Subtropical Front over the Chatham Rise, New Zealand. *New Zealand Journal of Marine and Freshwater Research*, 35: 1-15.
- , 2002. Temperature and salinity mean and variability within the Subtropical Front over Chatham Rise, New Zealand. *New Zealand Journal of Marine and Freshwater Research*, 36: 281-298.
- CHISWELL, S.M. and SUTTON, P.J.H., 1998. A deep eddy in the Antarctic Intermediate Water north of the Chatham Rise. *Journal of Physical Oceanography*, 28: 535-540.
- CLARKE, A., CHURCH, J. and GOULD, J., 2001. In: Siedler, G., Church, J. and Gould, J., Eds., *Ocean circulation and climate: observing and modelling the global ocean*, 11-30. San Diego: Academic Press.
- CORTESE, G., 2004. The 300 specimens problem. *Radiolaria: Newsletter of the international association of radiolarian paleontologists*, 22: 13-18.
- CORTESE, G. and ABELMANN, A., 2002. Radiolarian-based paleotemperatures during the last 160 kyr at ODP Site 1089 (Southern Ocean, Atlantic Sector). *Palaeogeography, Palaeoclimatology, Palaeoecology*, 182: 259-286.
- CRUNDWELL, M., SCOTT, G., NAISH, T., and CARTER, L., in press. Glacial-interglacial ocean climate variability during the Mid-Pleistocene transition in the temperate Southwest Pacific, ODP Site 1123. *Palaeogeography, Palaeoclimatology, Palaeoecology*
- DOLVEN, J.K., CORTESE, G. and BJØRKLUND, K.R., 2002. A high-resolution radiolarian derived paleotemperature record for the Late Pleistocene-Holocene in the Norwegian Sea. *Paleoceanography*, 17(4): 1072, 13 pp.
- DOW, R.L., 1978. Radiolarian distribution and the Late Pleistocene history of the Southeastern Indian Ocean. *Marine Micropaleontology*, 3(3): 203-227.
- DWORETZKY, B.A. and MORLEY, J.P., 1987. Vertical distribution of radiolaria in the Eastern equatorial Atlantic: analysis of multiple series of closely-spaced plankton tows. *Marine Micropaleontology*, 12: 1-19.
- FENNER, J., CARTER, L. and STEWART, R., 1992. Late Quaternary paleoclimatic and paleoceanographic change over northern Chatham Rise, New Zealand. *Marine Geology*, 108: 383-404.
- FENNER, J. and DI STEFANO, A., 2004. Late Quaternary oceanic fronts along Chatham Rise indicated by phytoplankton assemblages, and refined calcareous nannofossil stratigraphy for the mid-latitude SW Pacific. *Marine Geology*, 205(1-4): 59-86.
- GODFREY, M.G., ROEBUCK, E.M. and SHERLOCK, A.J., 1988. *Concise Statistics*. London: Edward Arnolds Publishers Ltd., 402 pp.
- HALL, I.R.; MCCAIVE, I.N.; SHACKELTON, N.J.; WEEDON, G.P. and HARRIS, S.E., 2001. Intensified deep Pacific inflow and ventilation in Pleistocene glacial times. *Nature*, 412: 809-812.
- HALL, I.R., CARTER, L. and HARRIS, S.E., 2002. Major depositional events under the deep Pacific inflow. *Geology*, 30(6): 487-490.
- HAMMER, Ø., HARPER, D.A.T. and RYAN, P.D., 2001. PAST: paleontological statistics Software Package for Education and Data Analysis. *Paleontologia Electronica*, 4(1): 9 pp. [hi/palaeo-electronica.org/2001_1/pasVissue1_01.].
- HAYS, J.D., 1965. Radiolaria and Late Tertiary and Quaternary history of Antarctic seas. In: LLANO, G.D., Ed. *Biology of the Antarctic Seas II*. American Geophysical Union, Antarctic Research Series, 5: 125-184.
- HAYS, J.D., IMBRIE, J. and SHACKLETON, N.J., 1976. Variations in the Earth's orbit: Pacemaker of the ice ages. *Science*, 194: 1121-1132.
- HAYS, J.D. and SHACKLETON, N.J., 1976. Globally synchronous extinction of the radiolarian *Stylatractus universus*. *Geology*, 4: 649-652.
- HAYS, J.D. and MORLEY, J.J., 2003. The Sea of Okhotsk: A Window on the Ice Age Ocean. *Deep-Sea Research I*, 50: 1481-1506.
- HAYWARD, B.W.; GRENFELL, H.R.; REID, C.M. and HAYWARD, K.A., 1999. Recent New Zealand shallow-water benthic foraminifera: Taxonomy, ecologic distribution, biogeography, and use in paleoenvironmental assessment. *Institute of Geological and Nuclear Sciences Monograph*, 21: 1-258.
- HEATH, R.A., 1976. Models of the diffusive-advective balance at the Subtropical Convergence. *Deep Sea Research*, 23: 1153-1164.
- , 1985. A review of the physical oceanography of the seas around New Zealand - 1982. *New Zealand Journal of Marine and Freshwater Research*, 19: 79-124.
- HOLLIS, C.J., MILDENHALL, D.C., CROUCH, E.M., and LÜER, V., 2002. Preliminary studies of palynomorphs and radiolarians from Quaternary marine sediment cores, offshore eastern New Zealand. *Institute of Geological and Nuclear Sciences file report 2002*, 2: 1-37.
- HOLLIS, C.J. and NEIL, H.L., 2005. Sedimentary record of radiolarian biogeography, offshore eastern New Zealand. *New Zealand Journal of Marine and Freshwater Research*, 39: 165-193.
- HOLLIS, C.J., NEIL, H.M., LÜER, V., SCOTT, G.H. and MANIGHETTI, B., 2006. Radiolarian-based sea-surface temperature estimates for the last 35,000 years, offshore eastern New Zealand. In: Lüer, V., Hollis, C.J., Campell, H. and Simes, J., Eds. *InterRad 11 and Triassic Stratigraphy Symposium; A joint international conference hosted by the International Association of Radiolarian Paleontologists, IGCP 467 and the Subcommission of Triassic Stratigraphy, 19-24 March 2006, Te Papa, Wellington, GNS Science miscellaneous series II*, Lower Hutt, Intitute of Geological and Nuclear Sciences Ltd: 85.
- HOWARD, W.R., 1997. A warm future in the past. *Nature*, 388: 418-419.
- ITAKI, T., 2003. Depth-related radiolarian assemblage in the water-column and surface sediments of the Japan Sea. *Marine Micropaleontology*, 47: 253-270.
- ITAKI, T. and HASEGAWA, S., 2000. Destruction of radiolarian shells during sample drying and its effect on apparent faunal composition. *Micropaleontology*, 46(1): 179-185.
- JACOT DES COMBES, H., CAULET, J.-P., and TRIBOVILLARD, N.P., 1999. Pelagic productivity changes in the equatorial area of the northwest Indian Ocean during the last 400,000 years. *Marine Geology*, 158: 27-55.

- JOHNSON, D.A. and NIGRINI, C., 1980. Radiolarian biogeography in surface sediments of the western Indian Ocean. *Marine Micropaleontology*, 5(2): 111-152.
- , 1982. Radiolarian biogeography in surface sediments of the eastern Indian Ocean. *Marine Micropaleontology*, 7(3): 237-281.
- JOSEPH, L.H., REA, D.K. and VAN DER PLUIJM, B.A., 2004. Neogene history of the Deep Western Boundary Current at Rekohu sediment drift, Southwest Pacific (ODP Site 1124). *Marine Geology*, 205: 185-206.
- KLING, S.A., 1979. Vertical distribution of polycystine radiolarians in the central north Pacific. *Marine Micropaleontology*, 4: 295-318.
- , 1998. Radiolaria. In: HAQ, B.U. AND BOERSMA, A., Eds. *Introduction to marine micropaleontology*, 203-244. New York: Elsevier Science.
- KLING, S.A. and BOLTOVSKOY, D., 1995. Radiolarian vertical distribution patterns across the southern California Current. *Deep Sea Research I*, 42(2): 191-231.
- LAZARUS, D.B., 1990. Middle Miocene to Recent radiolarians from the Weddell Sea, Antarctica, ODP Leg 113. In: barker, P.F., kennett, J.P., et al., Eds., *Proceedings of the Ocean Drilling Program, Scientific Results, Leg 113*. Ocean Drilling Program, College Station, Texas, A&M University, 113: 709-727.
- , 1992. Antarctic Neogene radiolarians from the Kerguelen Plateau, ODP legs 119 and 120. In: Wiese, S.W. and Schlich, R., Eds. *Proceedings of the Ocean Drilling Program, Scientific Results, Leg 20*, Ocean Drilling Program, College Station, Texas, A&M University, 20: 785-810.
- LING, H.-Y., 1974. Polycystine Radiolaria and silicoflagellates from surface sediments of the Sea of Okhotsk. *Bulletin of the Geological Survey of Taiwan*, 24: 1-11.
- LOMBARI, G. AND BODEN, G., 1985. Modern Radiolarian Global distributions. *Cushman Foundation for Foraminiferal Research, Special Publication*, 16A: 125 pp.
- LÜER, V., 2003. *Quaternary radiolarians from offshore eastern New Zealand, Southwest Pacific (ODP Leg 181, Site 1123): importance for correlation and identification of climatic changes*. Diploma Thesis, University of Bremen, Bremen, 105 pp., 11 pls., pdf [http://www-user.uni-Bremen.de/~micropal/lueer_de.htm].
- LÜER, V., HOLLIS, C.J. AND WILLEMS, H., 2006. Late Quaternary radiolarian assemblages as indicators for paleoceanographic changes north of the Subtropical Front, offshore eastern New Zealand, southwest Pacific. In: Lüer, V., Hollis, C.J., Campell, H. and Simes, J., Eds. *InterRad II and Triassic Stratigraphy Symposium; A joint international conference hosted by the International Association of Radiolarian Paleontologists, IGCP 467 and the Subcommission of Triassic Stratigraphy, 19-24 March 2006, Te Papa, Wellington*, 85. GNS Science miscellaneous series II. Lower Hutt: Institute of Geological and Nuclear Sciences Ltd.
- MARTINEZ, J.I., 1994. Late Pleistocene paleoceanography of the Tasman Sea: implications for the dynamics of the warm pool in the western Pacific. *Palaeogeography, Palaeoclimatology, Palaeoecology*, 112: 19-62.
- MCMILLEN, K.J. and CASEY, R.E., 1978). Distribution of living radiolarians in the Gulf of Mexico and Caribbean Sea, and comparison with the sedimentary record. *Marine Micropaleontology*, 3: 121-145.
- MOLINA-CRUZ, A., 1977. Radiolarian assemblages and their relationship to the oceanography of the subtropical southeastern Pacific. *Marine Micropaleontology*, 2:315-352.
- MOORE, T.C., 1973. Method of randomly distributing grains for microscopic examination. *Journal of Sedimentary Petrology*. 43(3): 904-906.
- , 1978. The distribution of radiolarian assemblages in the modern and ice-age Pacific. *Marine Micropaleontology*, 3: 229-266.
- MORLEY, J.J., 1979. A transfer function for estimating paleoceanographic conditions based on deep-sea surface sediment distribution of radiolarian assemblages in the South Atlantic. *Quaternary Research*, 12(3): 381-395.
- MORLEY, J.J. and HAYS, J.D., 1979. Cycladophora davisiana: a stratigraphic tool for Pleistocene north Atlantic and Interhemispheric correlation. *Earth and Planetary Science Letters*, 44: 383-389.
- , 1983. Oceanographic conditions associated with high abundances of the radiolarian Cycladophora davisiana. *Earth and Planetary Science Letters*, 66: 63-72.
- MORLEY, J.J. and SHACKLETON, N.J., 1978. Extension of the radiolarian *Strylactrus universus* as a biostratigraphic datum to the Atlantic Ocean. *Geology*, 6: 309-311.
- MORLEY, J.J. and STEPIEN, J.C., 1985. Antarctic Radiolaria in late winter/early spring Weddell Sea waters. *Micropaleontology*, 31(4): 365-371.
- MORLEY, J.J., TIASE, V.L., ASHBY, M.M. and KASHGARIAN, M., 1995. A high resolution stratigraphy for Pleistocene sediments from North Pacific sites 881, 883, and 887 based on abundance variations of the radiolarian *Cycladophora davisiana*. In: Rea, D.K., Basov, I.A., Scholl, D.W. and Allan, J.F., Eds., *Proceedings of the Ocean Drilling Program, Scientific Results, Volume 145*, 133-140. Ocean Drilling Program, College Station, Texas: A&M University.
- NAKASEKO, K. and NISHIMURA, A., 1982. Radiolaria from the Bottom Sediments of the Bellingshausen Basin in the Antarctic Sea. *Report of the Technology Research Center, J.N.O.C.*, 16: 91-244.
- NELSON, C.S., COOKE, P.J., HENDY, C.H., and CUTHBERTSON, A.M., 1993. Oceanographic and climatic changes over the past 160,000 years at Deep Sea Drilling Site 594 off southeastern New Zealand, southwest Pacific Ocean. *Paleoceanography*, 8: 435-458.
- NELSON, C.S., HENDY, I.L., NEIL, H.L., HENDY, C.H., and WEAVER, P.P.E., 2000. Late Glacial jetting of cold waters through the Subtropical Convergence zone in the Southwest Pacific off eastern New Zealand, and some geological implications. *Palaeogeography, Palaeoclimatology, Palaeoecology*, 156: 103-121.
- NIGRINI, C., 1977. Tropical Cenozoic Artostrobiidae. [Radiolaria]. *Micropaleontology*, 23(3): 241-269.
- NIGRINI, C.A. and MOORE, T.C., 1979. A guide to modern Radiolaria. *Cushman Foundation for Foraminiferal Research, Special Publication*, 16: i-xii, S 1-S 142, N1-N106, 28 pls.
- NIMMERGUT, A. and ABELMANN, A., 2002. Spatial and seasonal changes of radiolarian standing stocks in the Sea of Okhotsk. *Deep-sea Research I*, 49: 463-493.
- PAHNKE, K. and SACHS, J.P., 2006. Sea surface temperatures of southern midlatitudes 0-160 kyr B.P. *Paleoceanography*, doi: 10.1029/2005PA001191.

- PETRUSHEVSKAYA, M.G., 1967. *Radiolarii otryadov Spumellaria I Nassellaria antarkticheskoi oblasti (Antarctic Spumellina and Nassellina radiolarians)*. In: *Issledovaniya Fauny Morei 4(12), Rezultaty Biologicheskikh Issledovaniy Sovetskoi Antarkticheskoi Ekspeditsii 1955 - 1958*, 3. Nauk, Zoologicheskii Institut Akademiya Nauk SSSR: 186 pp.
- , 1971a. Radiolaria in the plankton and recent sediments from the Indian Ocean and Antarctic. In: Funnell, B.M. and Riedel, W.R., Eds., *The Micropalaeontology of Oceans*, 319-329. London: Cambridge University Press.
- , 1971b. Spumellarian and nassellarian radiolaria in the plankton and bottom sediments of the central Pacific. In: Funnell, B.M. and Riedel, W.R., Eds., *The Micropalaeontology of Oceans*, 309-317. London: Cambridge University Press.
- , 1975. Cenozoic radiolarians of the Antarctic, Leg 29, DSDP. In: Kennett, J.P., Hourz, R.E., et al., Eds., *Initial Reports of the Deep Sea Drilling Project, Volume 29*, 541-675. Washington DC, US Government Printing Office.
- PETRUSHEVSKAYA, M.G. and KOSLOVA, G.E., 1972. Radiolaria: Leg 14. Deep Sea Drilling Project. In: Hayes, D.E., Pimm, A.C. et al., Eds. *Initial Reports of the Deep Sea Drilling Project, Volume 14*, 495-648. Washington, DC: US Government Printing Office.
- PISIAS, N.G. and MIX, A.C., 1997. Spatial and temporal oceanographic variability of the eastern equatorial Pacific during the Late Pleistocene: Evidence from Radiolaria microfossils. *Paleoceanography*, 12: 381-393.
- RENZ, G.W., 1976. The distribution and ecology of Radiolaria in the central Pacific: Plankton and surface sediments. *Bulletin of the Scripps Institution of Oceanography of the University of California*, 22: 1-262.
- SANFILIPPO, A., WESTBERG-SMITH, M.J. and RIEDEL, W.R., 1985. Cenozoic Radiolaria. In: Bolli, H.M., Saunders, J.B. and Perch-Nielsen, K., Eds., *Plankton Stratigraphy*, 631-712. London: Cambridge University Press.
- SANFILIPPO, A. and NIGRINI, C., 1998. Code numbers for Cenozoic low latitude radiolarian biostratigraphic zones and GPTS conversion tables. *Marine Micropaleontology*, 33: 109-156.
- SHACKLETON, N.J., and HALL, M.A., 1989. Stable isotope history of the Pleistocene at ODP Site 677. In: BECKER, K., SAKAI, H. et al., Eds. *Proceedings of the Ocean Drilling Program, Scientific Results, Volume 111*, 295-316., College Station, Texas: Ocean Drilling Program.
- SHACKLETON, N.J., BALDAUF, J.G., FLORES, J.-A., IWAI, M., MOORE, T.C., RAFFI, I. and VINCENT, E., 1995. Biostratigraphic summary for Leg 138. In: Pisias, N.G., Mayer, L.A., Janecek, T.R., Palmer-Julson, A. and Van Andel, T.H., Eds. *Proceedings of the Ocean Drilling Program, Scientific Results, Volume 138*, 517-536., College Station, Texas: Ocean Drilling Program.
- SIKES E.L., HOWARD, W.R., NEIL, H.L. AND VOLKMANN, J.K., 2002. Glacial-interglacial sea surface temperature changes across the subtropical front east of New Zealand based on alkenone unsaturation ratios and foraminiferal assemblages. *Paleoceanography*, 17(2): 1012, 10.1029/2001PA000640, 2002.
- SUTTON, P.J.H., 2003. The Southland Current: a subantarctic current. *New Zealand Journal of Marine and Freshwater Research*, 37: 645-652.
- TAKAHASHI, K., 1991. Radiolaria: Flux, Ecology, and Taxonomy in the Pacific and Atlantic. *Ocean Biocoenosis Series*, 3: 1-303.
- TAKAHASHI, K. AND HONJO, S., 1981. Vertical flux of Radiolaria: A taxon-quantitative sediment trap study from the western tropical Atlantic. *Micropaleontology*, 27(2): 140-190.
- WANG, R. AND ABELMANN, A., 2002. Radiolarian responses to paleoceanographic events of the southern South China Sea during the Pleistocene. *Marine Micropaleontology*, 46: 25-44.
- WARREN, B.A., 1981. Deep circulation of the world ocean. In: Warren, B.A. and Wunsch, C., Eds., *Evolution of Physical Oceanography*, 6-41. Cambridge: Massachusetts Institute of Technology Press.
- WEINHEIMER, A.L., 2001. Radiolarians from Northern Cape Basin, Site 1082. In: WEFER, G., BERGER, W.H. AND RICHTER, C., Eds. *Proceedings of the Ocean Drilling Program, Scientific Results, Volume 175*, 1-16., College Station, Texas: Ocean Drilling Program. [http://www-odp.tamu.edu/publications/175_SR/VOLUME/CHAPTERS/SR175_03.PDF].
- WELLING, L.A., PISIAS, N.G. and ROELOFS, A.K., 1992. Radiolarian microfauna in the northern California Current System: indicators of multiple processes controlling productivity. In: Summerhayes, C.P., Prell, W.L. and Emeis, K.C., Eds., *Upwelling Systems. Evolution since the Early Miocene*, 177-195. London Geological Society: Geological Society Special Publication, 64.
- WELLING, L.A., PISIAS, N.G., JOHNSON, E.S., and WHITE, J.R., 1996. Distribution of polycystine radiolaria and their relation to the physical environment during the 1992 El Nino and following cold event. *Deep-Sea Research II*, 43(4-6): 1413-1434.
- WELLING, L.A. and PISIAS, N.G., 1998. How do radiolarian sediment assemblages represent surface ocean ecology in the central equatorial Pacific?. *Paleoceanography*, 13(2): 131-149.
- YAMASHITA, H., TAKAHASHI, K. and FUJITANI, N., 2002. Zonal and vertical distribution of radiolarians in the western and central Equatorial Pacific in January 1999. *Deep-Sea Research II*, 49: 2823-2862.

Site 1123: Samples were processed using a standard method for preparation of Cenozoic radiolarians (Sanfilippo et al. 1985) incorporating the >63 µm size fraction and using a hand strewn dry method for producing microscope slides, including oven drying of bulk sediments and residues. Sample processing and slide preparation were as followed:

1. Bulk sediment samples are oven-dried (40°C), weighed and transferred into 600 ml glass beakers.
2. 100-150 ml 10% HCl, 20 ml 30% HCl is slowly added.
3. The sediment residue is washed through a 63µm screen, transferred into a 250 ml glass beaker adding a 4:1 solution of 10% H₂O₂ and 5% Na(PO₃)₆, covered with a watchglass while heated and simmered on the hot plate (~1 hour).
4. The clean residue is washed through a 63µm screen, transferred into a 250 ml glass beaker, oven-dried (40°C) and transferred into a waxed paper holder.
5. For radiolarian strewn slide preparation dilute gum tragacanth base is painted on a cover slip-seized central area of a cleaned glass slide and left to dry; slides are labelled and laid out on a waxed paper.
6. Dried residue is sprinkled regularly over the tragacanthed part of the glass slide, the slide is breathed on carefully to making the slide sticky.
7. Two drops of xylene are placed in the centre of the slide using a glass pipette and slowly, 20-25 drops of Entellan-Neu are placed on the residue using a disposable dropper and a cover slip is placed onto the residue.
8. Placed in a flat warm well-ventilated spot the mounting medium hardens in five days.

Site 1124: Samples were freeze-dried and processed (Abelmann 1988). The retrieved >45 µm fraction was transferred to the microscope slides by using a wet settling technique adopted from Moore (1973); Abelmann (1988) and Abelmann et al. (1999). Radiolarian residues were mounted in Norland applying a newly developed quick, cold mounting technique which ensured the production of microscope slides without significant numbers of air bubbles,

especially within radiolarian tests. Formation of bubbles in the matrix and within radiolarian tests has been a longstanding problem with Norland (C. A. Nigrini; K. R. Bjørklund; written communications, 2004). The cold use of xylene was found to be an effective way of avoiding formation of air bubbles. Sample processing and slide preparation methods are specified below.

1. Samples are deep-frozen, freeze-dried, weighed and transferred into a 600 ml glass beaker.
2. The sediment is covered with some demineralized water, 100 ml of a 4:1 solution of 10% H_2O_2 and 5% $\text{Na}(\text{PO}_3)_6$ and 100 ml 10% HCl are slowly added while simmering on the hot plate for ~1 hour.
3. The glass beaker is filled up to 600 ml with demineralized water, the residue is washed through a 45 μm mesh and transferred into a 50 ml centrifuge plastic tube and kept in solution with demineralized water.
4. A rectangular plastic settling container (95 x 45 x 45 mm) is filled with a 1:2.5 solution of gelatine and water before three clean cover slips (40 x 22 mm) are aligned on the bottom of the container.
5. An automatic pipette is used to evenly distribute a defined amount of suspension which depends on the size of the residue (generally 5-10 ml) into the liquid-filled settling container.
6. After allowing all particles to sink and settle on the cover slips (~2 hours) a siphoning system is used to remove most of the liquid from the container. Soft paper strips are hung into the liquid to slowly remove the remaining water without creating convection.
7. Dry cover slips are removed from the settling container, using a razor blade.
8. For preparation of radiolarian strewn slides the residue-coated cover slip is placed on a cool, flat surface, 2-3 drops of xylene are dropped on the residue using a glass pipette to remove air pockets within and between tests.
9. Once the inter-particle area is dry but the residual grains are still wet, ~10 drops of Norland are slowly placed on each cover slip to be mounted on glass slides; evaporation of xylene occurs at room temperature without the use of heat, e.g. from a hot plate.
10. After ~20 minutes of UV light treatment the mounting medium is hardened and slides are ready for microscopic analysis.